Chapter VI

LABORATORY INVESTIGATIONS

6.0 INTRODUCTION

The contents of this chapter reflects the observations pertaining to the detail laboratory investigations carried out for the representative samples of the various lithological units exposed within the Quaternary successions along the Kim, Tapi and Mindhola river valleys. The various laboratory techniques adopted in the present study includes the hand specimen observations under binocular microscope, granulometric analyses of arenaceous sediments, X-ray diffraction studies for mineralogical details, scanning electron microscope studies for surface morphological attributes, geochemical investigations for trace element concentrations and micro-palaeontological analyses. The results obtained from the laboratory investigations have been interpreted and integrated to understand the influence of various processes during

the deposition of Quaternary sediments within the study area. The succeeding pages of this chapter provide the detailed account of each of the laboratory techniques employed in the present work and their results so obtained.

6.1 GRANULOMETRIC ANALYSIS

The granulometric analysis deals with the grain size measurements of particles ranging from granule to fine sand (Sengupta, 1994). The grain size parameters reciprocates with the factors like availability of source materials, medium of transport, winds, waves, climate, long shore currents along with physiography and geomorphology of an area (King, 1972; Swift, 1976). These parameters, in various combinations aptly indicates the nature of processes responsible for the transportation and deposition of the sediments (Friedman, 1961) and thereby widely used for environmental differentiation (Mason & Folk, 1958; Friedman, 1961, 1962 & 1967; Moiola & Weiser, 1968; Solohub & Klovan, 1970) and also to understand the processes that form the clastic sediments (Inman, 1949 & 1952; Passega, 1957; Folk & Ward, 1957; Stewart, 1958; Friedman, 1961 & 1967; Moiola & Weiser, 1968; Gleister & Nelson, 1974; Sahu, 1964 and 1983).

In the present study, the granulometric analyses has been carried out for 27 representative samples belonging to the various sand units (2mm to 62.5μm), following the standard technique of Carver (1971). Individual sample was subjected for sieving using ASTM (American Society for Testing Materials) sieve set of half phi interval, for about 10 minutes on a Ro – Tap mechanical shaker. The size fractions obtained in the sieves were weighed individually to the nearest 0.001gm to obtain grain size frequency distribution. The particle size distribution data thus obtained were graphically represented in the form of standard curves suggested by Folk (1974).

The various statistical parameters (Table 6.1) were computed using the formulas of Folk and Ward (1957) and are given below, where, Φ_5, Φ_{16}, Φ_{50} etc. are the grain size in phi units (-$\log_2$ of grain size in mm) corresponding to the 5th, 16th, 50th etc. percentile on the cumulative curve of grain size distribution.

	Statistical Measure		*Formula*
i.	Mean Diameter (M_Z)	=	$(\Phi_{16} + \Phi_{50} + \Phi_{84})/3$
ii.	Inclusive Graphic Standard Deviation (σ_1)	=	$\{(\Phi_{84} - \Phi_{16})/4\} + \{(\Phi_{95} - \Phi_5)/6.6\}$
iii.	Inclusive Graphic Skewness (SK_1)	=	$\{(\Phi_{16} + \Phi_{84} - 2\Phi_{50})/ 2(\Phi_{84} - \Phi_{16})\} + \{(\Phi_5 + \Phi_{95} - 2\Phi_{50})/ 2(\Phi_{95} - \Phi_5)\}$
iv.	Graphic Kurtosis (K_G)	=	$(\Phi_{95} - \Phi_5)/ 2.44(\Phi_{75} - \Phi_{25})$

6.1.1 Kim River

The lithological successions observed at various locations along the Kim river represent three cycles of fining upward sequences. Overall, six representative samples of sands belonging to the different cycles were treated for granulometric analysis, the details of which are discussed below.

[I] Grain Size Parameters –

(a) Graphic Mean (M_Z): The Graphic Mean (M_Z) represents the average size of the sediments (Folk, 1974). The M_Z value obtained for the sample (KmB1C) belonging to first cycle of sedimentation is -0.49Φ, indicating very coarse sand size however, the values for the remaining five samples (KmB1E, KmB1F, KmB1G, KmB2A and KmB4D) belonging to the third cycle of sedimentation ranges from -0.13Φ to 0.96Φ with an average of 0.32Φ, indicating coarse sand size.

River	Cycle	Sample No.	ϕ							Grain Size Parameters			
			ϕ5	ϕ16	ϕ25	ϕ50	ϕ75	ϕ84	ϕ95	M_Z	σ1	SK_I	K_G
Kim	III	KmB1E	-1.75	-1.35	-1.04	-0.39	0.24	1.36	3.57	-0.13	1.48	0.39	1.70
		KmB1F	-1.35	-0.46	-0.17	0.46	1.16	1.63	3.16	0.54	1.21	0.16	1.39
		KmB1G	-0.77	0.11	0.38	0.97	1.52	1.80	3.21	0.96	1.03	0.05	1.43
		KmB2A	-3.50	-2.09	-1.42	0.06	1.21	1.77	3.28	-0.09	1.99	-0.08	1.06
		KmB4D	-1.92	-1.34	-1.04	-0.11	1.62	2.41	3.71	0.32	1.79	0.35	0.87
	I	KmB1C	-2.27	-1.68	-1.39	-0.56	0.41	0.76	2.69	-0.49	1.36	0.20	1.13
Tapi	IV	TB3e	-3.10	-2.35	-2.00	-1.08	0.11	0.67	2.50	-0.92	1.60	0.22	1.09
	III	TB1B	-2.50	-1.60	-0.74	-0.15	0.55	0.88	1.91	-0.29	1.29	-0.12	1.40
		TB5E	0.40	1.12	1.47	1.76	2.60	3.08	4.04	1.79	1.04	0.30	1.32
	II	TB2B	-3.98	-1.82	-0.76	1.02	1.66	1.97	2.62	0.39	1.95	-0.51	1.12
		TB3B	-2.40	-1.26	-0.72	0.68	2.61	3.28	4.24	0.90	2.14	0.11	0.82
		TB6C	-2.36	-1.50	-0.84	0.74	2.06	2.50	3.34	0.58	1.86	-0.10	0.81
	I	TB3a	-3.55	-2.63	-2.18	-1.22	-0.26	0.20	1.28	-1.22	1.44	0.02	1.03
		TB3A	-1.92	-1.04	-0.57	0.06	0.66	0.96	1.67	-0.01	1.04	-0.10	1.20
		TB4E	-2.18	-1.50	-0.98	0.18	1.49	2.14	3.45	0.59	1.76	0.12	0.93
Mindhola	IV	MB3F	-2.25	-1.48	-1.06	-0.30	0.30	0.60	1.14	-0.39	1.03	-0.14	1.02
		MB3G	1.76	2.06	2.20	2.51	2.82	2.98	3.39	2.52	0.48	0.05	1.08
		MB4B	-0.77	0.71	1.24	1.84	2.40	2.74	3.32	1.76	1.13	-0.19	1.45
		MB4C	-3.86	-2.42	-1.72	-0.21	1.25	1.94	3.04	-0.23	2.14	-0.04	0.95
		MB5E	-1.86	-0.87	-0.15	0.95	1.70	2.04	2.76	0.71	1.43	-0.23	1.02
		MB5F	-5.94	-4.78	-4.22	-3.01	-1.84	-0.79	3.98	-2.86	2.50	0.26	1.71
		MB7I	0.09	1.00	1.35	1.71	1.96	2.29	3.08	1.67	0.78	-0.09	2.01
		MB7J	-1.56	0.69	0.99	1.60	2.22	2.52	3.12	1.60	1.17	-0.17	1.56
	III	MB5J	-2.48	-1.76	-1.36	-0.04	1.24	2.30	3.74	0.17	1.96	0.18	0.98
	II	MB3A	-5.50	-4.21	-3.56	-2.22	-0.88	-0.24	1.05	-2.22	1.98	0.00	1.00
		MB6C	-1.98	-1.10	-0.39	0.66	1.35	1.68	2.36	0.41	1.35	-0.24	1.02
		MB7B	-3.64	-2.69	-2.28	-1.25	0.61	1.50	3.25	-0.81	2.09	0.31	0.98

Table 6.1 – Granulometric Analyses Of Quaternary Sand Samples Exposed Along The Kim, Tapi And Mindhola Rivers.

(b) The Standard Deviation (σ_I): The Standard Deviation (σ_I) measures the sorting of sediments and indicate the fluctuations in the kinetic energy (velocity) conditions of the depositing agent with respect to its average velocity (Sahu, 1964). The σ_I value of the sediment belonging to first cycle is 1.36Φ, which indicates a poorly sorted nature. The sediments belonging to third cycle show σ_I value ranging from 1.03Φ to 1.99Φ with an average of 1.51Φ, also indicating a poorly sorted nature.

(c) The Inclusive Graphic Skewness (SK_I): The Inclusive Graphic Skewness (SK_I) measures the degree of asymmetry of the frequency distribution and marks the position of the mean with respect to the median. If the skewness is negative, the sample is coarsely skewed, indicating that the mean is towards the coarser side of the median (Sahu, 1964).

The SK_I value for the sediment of first cycle is 0.20 indicating a fine-skewed nature whereas the values for sediments of third cycle show a range from -0.08 to 0.39 with an average of 0.174, indicating an overall fine-skewed nature.

(d) The Graphic Kurtosis (K_G): The Graphic Kurtosis (K_G) measures the ratio between the sorting in the "tails" (90%) of the curve and the sorting in the central portion (50%) (Folk, 1974). The K_G value obtained for the arenaceous sediments of first cycle is 1.13, and those for the third cycle sediments range from 0.87 to 1.70 with an average of 1.29, indicating an overall leptokurtic nature.

[II] Grain Size Distribution Curves –

The distribution of particle size in sediments is a function of the availability of different sizes of particles in the parent material and the processes operating where the particles were deposited (Friedman and Johnson, 1982). In order to understand the grain size distribution of

the Quaternary sediments, the sieving data has been represented graphically in the form of frequency distribution curve and cumulative-frequency distribution curves.

The grain size frequency distribution curve of sediment belonging to the first cycle show a large proportion of coarser sediments (Fig. 6.1a), with small amount of the pan-fractions (~2%). The primary mode of the curve is at 0.0Φ while the secondary mode lies at -1.0Φ. In the case of sediments belonging to third cycle also, the grain size frequency distribution curves show comparatively large proportion of coarse sand size particles and small proportion of pan-fractions (<3%). The primary mode of grain size distribution curve lies between 0.0Φ to 1.0Φ, whereas the secondary mode lies at 2.5Φ (Fig. 6.2a).

The cumulative frequency size distribution curve of the sediment belonging to first cycle (Fig. 6.1b) shows two truncation points, i.e., between suspension and saltation loads and between saltation and surface creep (traction) loads. It is evident from this curve that the traction load is about 40% by weight of the sample, which are deposited by rolling or sliding motion. The saltation fraction, which shows two sub-populations, comprises around 55% whereas the suspension load constitutes less than 5% by weight of the sample. The two sub-populations observed within the saltation population are represented by two separate straight line segments probably differentiated by slope dependent sorting values (Friedman and Johnson, 1982). The above observations indicate that majority of the sediments have either moved by jumping motion or by rolling and sliding motion with minor proportions carried in suspension. The truncation point between suspension and bed load transport lies at 3.5Φ, while the truncation point between saltation and traction lies at -1.0Φ. In the case of sediments belonging to the third cycle, the cumulative frequency size distribution curves (Fig. 6.2b) show two different natures; one with a single saltation population, as shown by the sample KmB1E and the other with two saltation sub-populations.

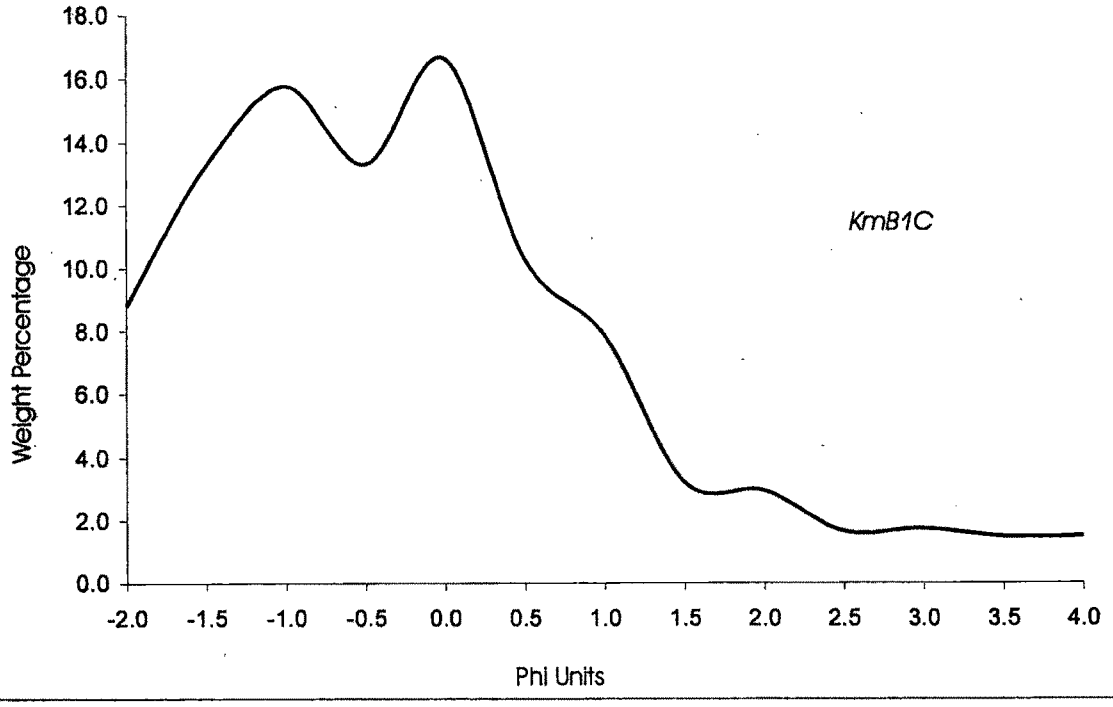

Fig. 6.1a - Diagram Showing The Frequency Curve Of Sediments Belonging To First Cycle Of Quaternary Succession (Loc:- Kim River).

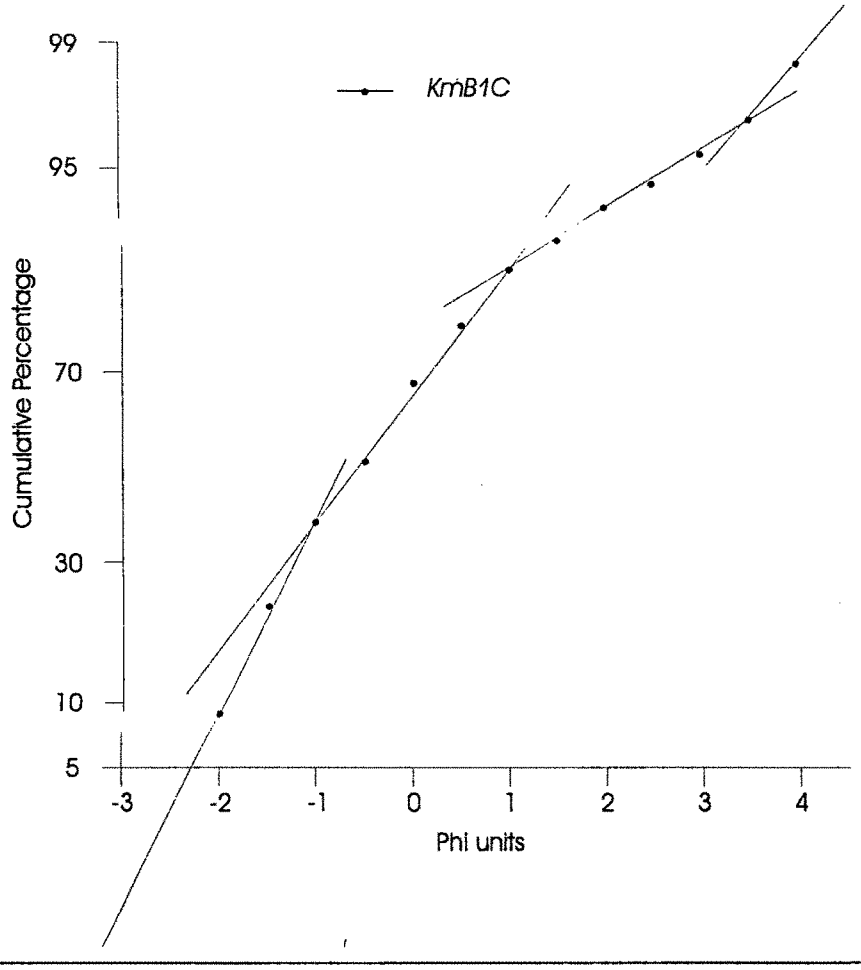

Fig. 6.1b - Diagram Showing The Cumulative Frequency Curve Of Sediments Belonging To First Cycle Of Quaternary Succession (Loc:- Kim River).

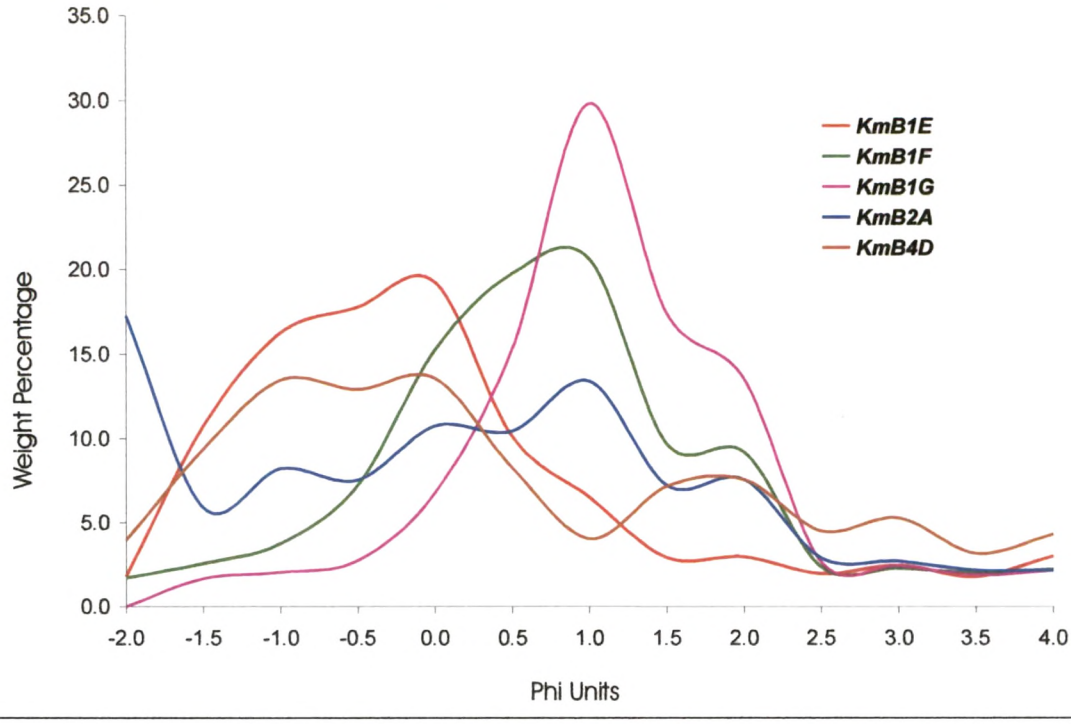

Fig. 6.2a - Diagram Showing The Frequency Curve Of Sediments Belonging To Third Cycle Of Quaternary Succession (Loc:- Kim River).

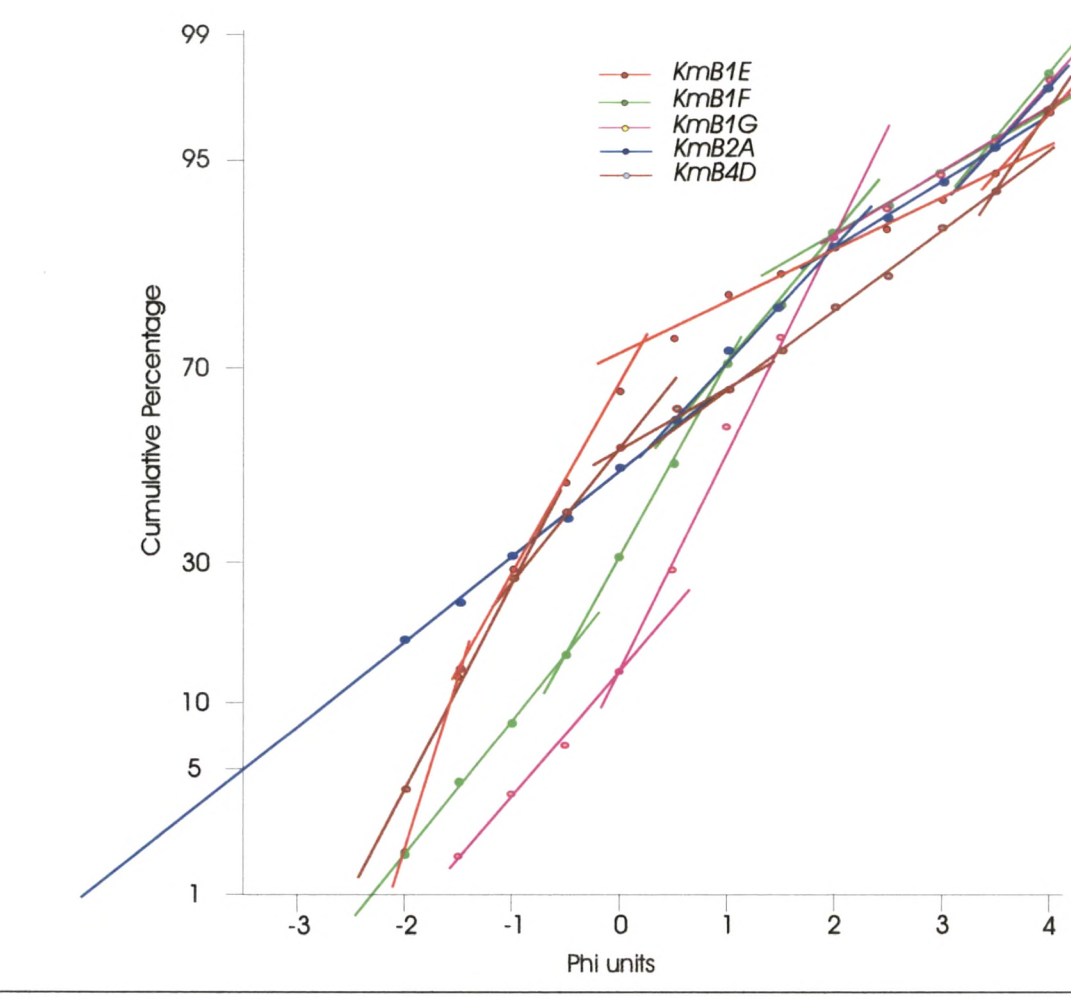

Fig. 6.2b - Diagram Showing The Cumulative Frequency Curve Of Sediments Belonging To Third Cycle Of Quaternary Succession (Loc:- Kim River).

It is observed that in all the samples traction population is more than 50% by weight of the sample, except, in the sample KmB1G, where the traction population is found to be about 15%. The saltation load is observed to be around 40 – 45% whereas the suspension load constitutes less than 5% by weight of the sample. The truncation point between suspension and saltation lies at 3.5Φ, while that between saltation and traction lies between -0.5Φ to 0.75Φ.

[III] Bivariant Discriminant Plots –

The Bivariant Discriminant plots are represented by scatter diagrams of two variables to distinguish between different environments of sediments deposition.

Moiola and Weiser (1968) have utilized the combinations of mean diameter (M_Z) vs. standard deviation (σ_I) and skewness (SK_I) vs. standard deviation (σ_I) to differentiate between the beach and river sands. Stewart (1958) has used the combination of standard deviation (σ_I) and median (50%) for discriminating between river and wave processes.

Gleister and Nelson (1974) have shown the gradational change of all the depositional system within a fluvial regime by constructing a bivariant plot between mean diameter (M_Z) and standard deviation (σ_I). Sahu (1964) adopted an empirical graph of $\sqrt{(\sigma_1)^2}$ vs. $\{(SK_G/SM_Z) \times S(\sigma_1)^2\}$ where, $(\sigma_1)^2$ is the variance, and SK_G, SM_Z and $S(\sigma_1)^2$ represents standard deviation of the graphic mean, graphic kurtosis and variance, on a log-log paper to discriminate between aeolian, marine, fluvial and turbidity current mechanisms.

The M_Z, σ_I and SK_I values obtained for the arenaceous sediments belonging to first and third cycle of the Quaternary successions of Kim river have been plotted in the above mentioned scatter diagrams. The plot suggested by Moiola and Weiser (1968), aptly indicates that the Quaternary sediments representing first and third cycles fall in the fluvial domain (Fig. 6.3).

The scatter diagram of Stewart (1958) indicates that these sediments have been transported and/or deposited by river processes (Fig. 6.4). The plot of Gleister and Nelson (1974) has shown that these sediments fall in the region between alluvial fan and braided bar (Fig. 6.5). The log – log plot of Sahu (1964) clearly indicates that the sediments belonging to third cycle, represents fluvial environment of deposition (Fig. 6.6).

[IV] C-M Plots –

Passega (1957, 1964), based on the grain size parameters, has proposed the C-M Plots, where C represents one percentile and M, the median diameter (50%), to understand the processes of transportation of sediments. The C-M plots obtained for the arenaceous sediments of the study area are depicted in figure 6.7.

These plots have shown that the sediments belonging to the Kim river sections occur above the ON segment, indicating their transport dominantly by rolling process.

6.1.2 Tapi River

The Quaternary cliff-sections exposed at various locations along the Tapi river, displays four cycles of fining upward sequences. A total of nine representative sand samples representing these cycles have been treated for granulometric analyses. The details of which are furnished below.

[I] Grain Size Parameters –

(a) Graphic Mean (M_Z): The M_Z values for the sediments belonging to first cycle (TB3a, TB3A & TB4E), ranges between -1.22Φ to 0.59Φ, with an average of -0.21Φ, indicating very coarse sand size.

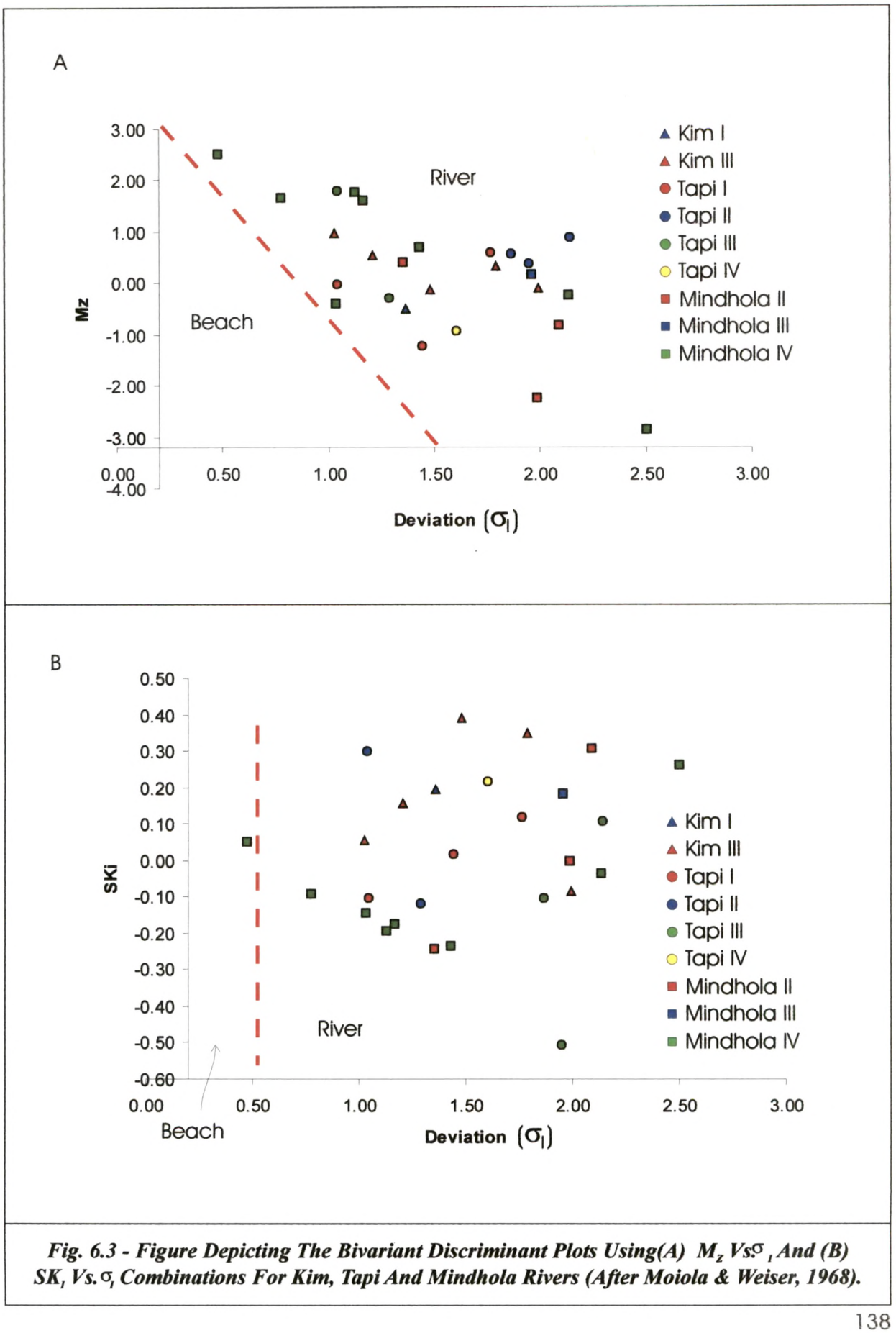

Fig. 6.3 - Figure Depicting The Bivariant Discriminant Plots Using(A) M_z Vs.σ_I And (B) SK_I Vs.σ_I Combinations For Kim, Tapi And Mindhola Rivers (After Moiola & Weiser, 1968).

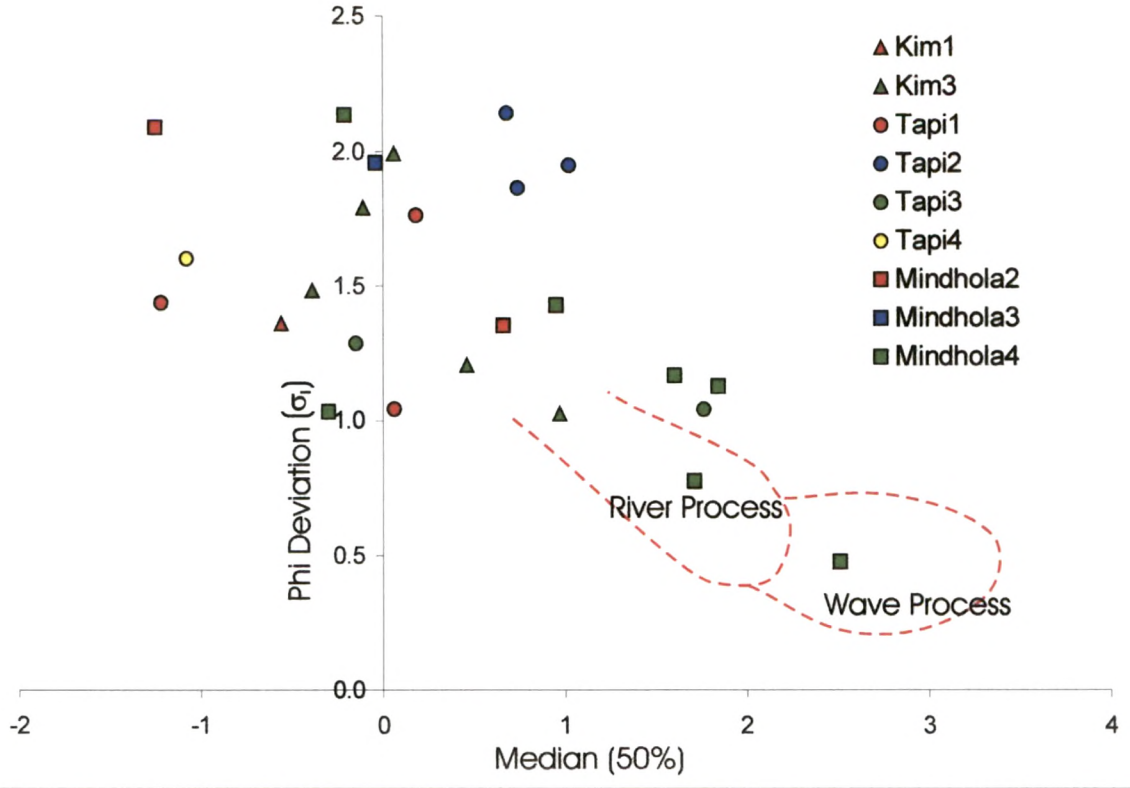

Fig. 6.4 - Figure Depicting The Bivariant Plots Ofσ_i Vs. Median Combinations For Sediments Of The Study Area (After Stewart, 1958).

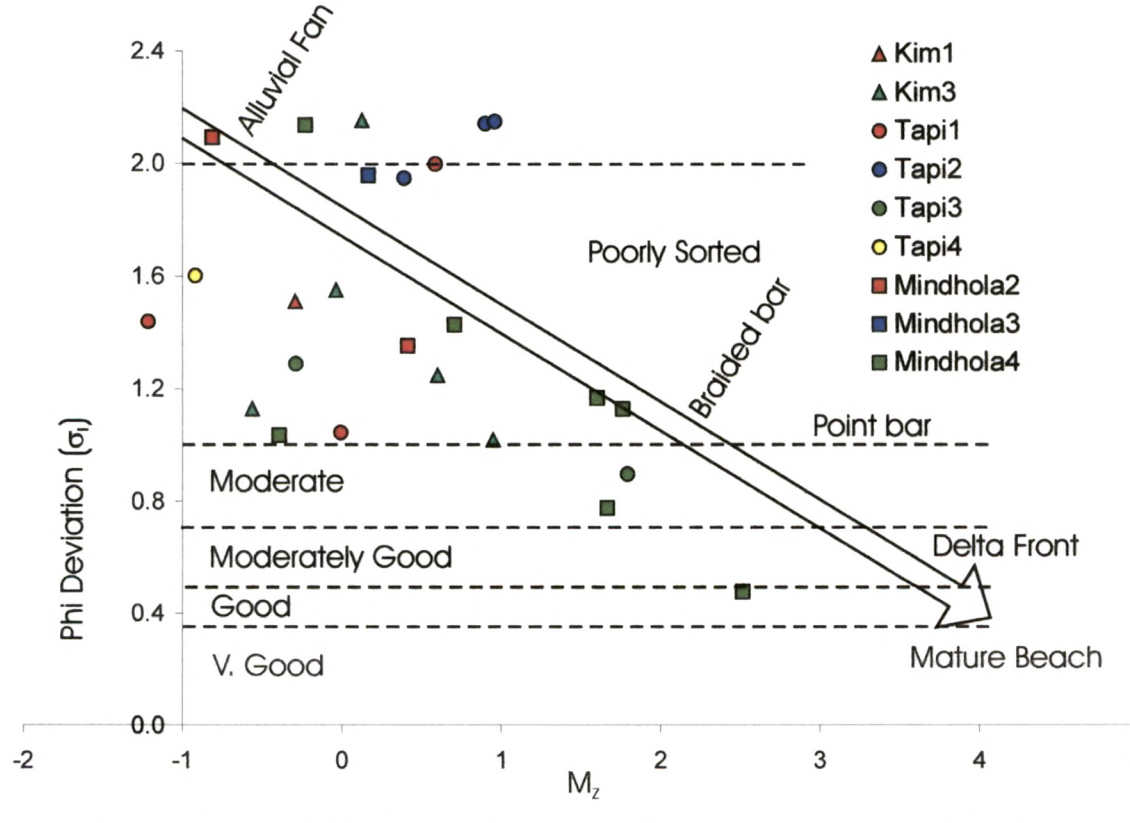

Fig. 6.5 - Figure Depicting The Bivariant Plots Using M_z Vsσ_i For Sediments Of The Study Area (After Gleister & Nelson, 1974).

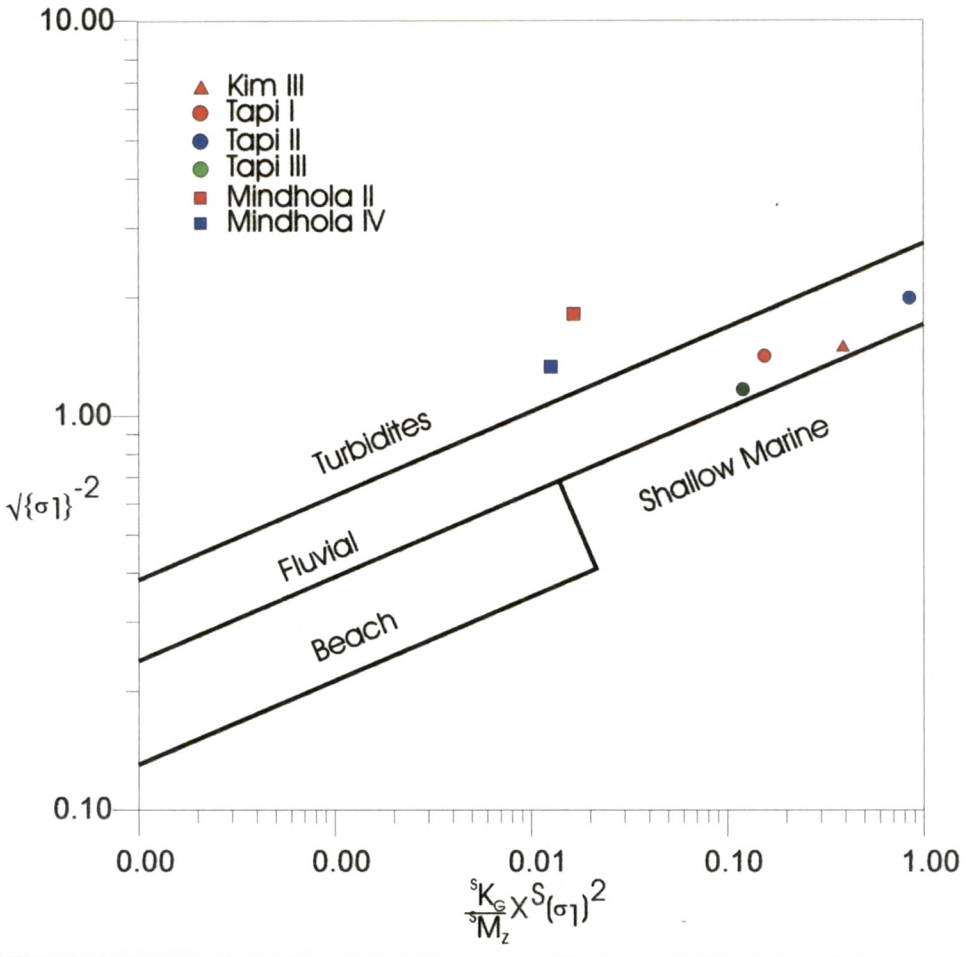

Fig. 6.6 - Figure Depicting The Log - Log Plot For The Sediments Of The Study Area (After Sahu, 1964).

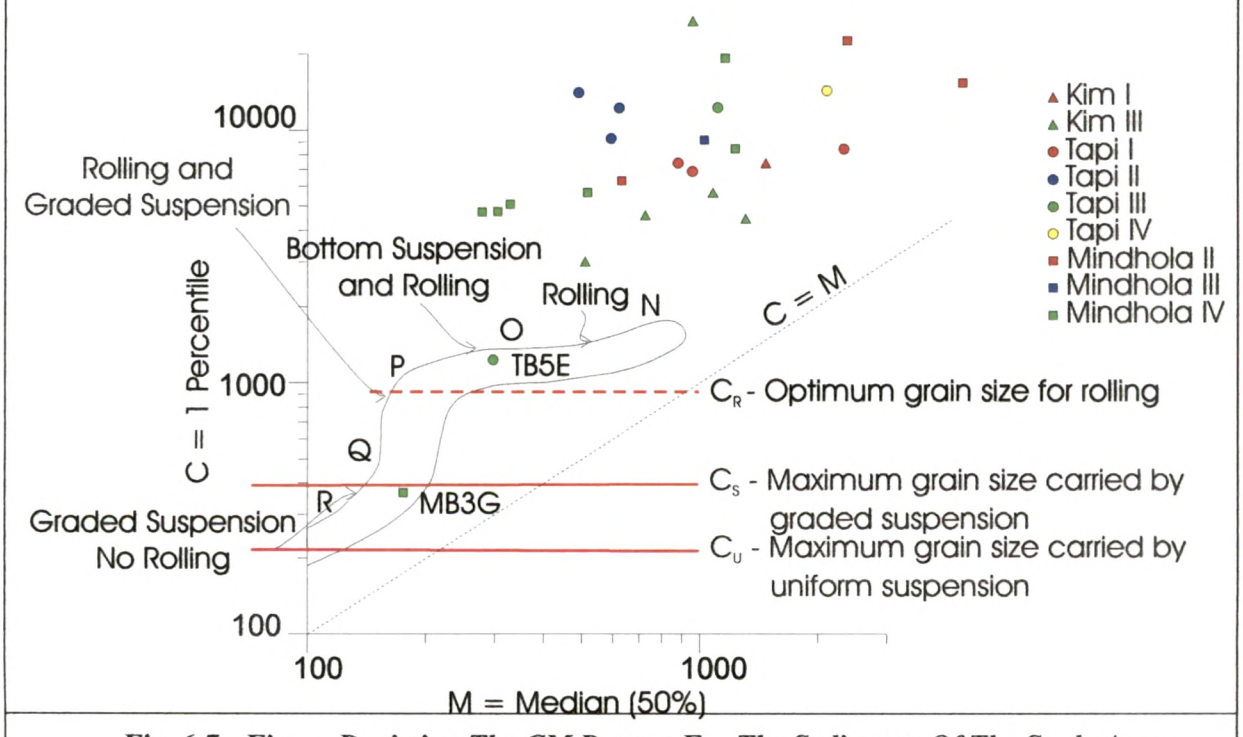

Fig. 6.7 - Figure Depicting The CM Pattern For The Sediments Of The Study Area (After Passega, 1964).

However, the M_Z values for the sediments belonging to second cycle (TB2B, TB3B & TB6C), range between 0.39Φ and 0.90Φ, with an average of 0.62Φ, thereby indicating a coarse sand size. The M_Z values for the sediments belonging to third cycle (TB1B & TB5E), vary between -0.29Φ and 1.79Φ, with an average of 0.75Φ, indicating again a coarse sand size. The M_Z value obtained for the sediment belonging to the fourth cycle (TB3e), is -0.92Φ, indicating a very coarse sand size.

(b) Standard Deviation (σ_I): The σ_I values for the sediments belonging to first cycle range between 1.04Φ to 1.76Φ with an average of 1.42Φ, indicating a poorly sorted nature. The sediments belonging to second cycle show higher values of σ_I ranging between 1.95Φ and 2.14Φ, with an average of 1.98Φ, indicating a very poorly sorted nature. The σ_I values for sediments belonging to third cycle ranges between 1.04Φ and 1.29Φ, with an average of 1.165Φ, indicating a poorly sorted nature. Similarly σ_I value for sediment belonging to fourth cycle is 1.60Φ again indicating poorly sorted nature.

(c) Inclusive Graphic Skewness (SK_I): The SK_I values for the sediments belonging to first cycle ranges between -0.10 and 0.12, with an average of 0.01, indicating a near symmetrical nature, whereas the SK_I values for the sediments belonging to second cycle range between -0.51 and 0.11 with an average of -0.167, indicating a coarse-skewed nature. The sediments belonging to third cycle show SK_I values ranging between -0.12 and 0.30, with an average of 0.09, indicating a near-symmetrical nature, while that belonging to the fourth cycle have 0.22 value, indicating a fine-skewed nature of the sediments.

(d) Graphic Kurtosis (K_G): The K_G values for the sediments belonging to first cycle range between 0.93 and 1.20, with an average of 1.05 while those belonging to second cycle show values ranging between 0.81 and 1.12 with an average of 0.91, overall indicating a mesokurtic nature. The K_G values of the sediments belonging to third cycle range between

1.32 and 1.4 with an average of 1.36, indicating a leptokurtic nature, however the sediment belonging to fourth cycle shows mesokurtic nature with a K_G value of 1.09.

[II] Grain Size Distribution Curves –

The grain size frequency distribution curves (Fig. 6.8a) of sand samples representing the first cycle, show dominance of coarser sediments and minor proportion of pan-fraction (<3%). The primary mode lies between 0.0Φ and 1.0Φ however, in case of sample (TB3a) the primary mode shows -2.0Φ value. The secondary mode lies between 1.5Φ to 2.0Φ. The sediments belonging to second cycle displays frequency distribution curves (Fig. 6.9a) with dominance of fine to medium sands, whereas the pan-fraction proportion varies from 1 to 7% by weight of the sediments. The primary mode lies between 0.0Φ and 2.0Φ, whereas the secondary mode lies at 3.0Φ. The frequency distribution curves (Fig. 6.10a) of the sediments belonging to third cycle show dominance of coarser and finer sands with pan-fraction varying from <1% to 4%. The primary mode ranges between 0.0Φ and 2.0Φ and the secondary mode lies between 2.0Φ and 3.0Φ. The sediment belonging to the fourth cycle shows frequency distribution curve exhibiting dominance of coarser sediments with pan-fraction (<2%). The primary mode of this curve lies at -2.0Φ, whereas the secondary mode lies at 0.0Φ (Fig. 6.11a).

The cumulative frequency size distribution curves (Fig. 6.8b) obtained for the sediments belonging to first cycle shows two truncation points, one between suspension and saltation and other between saltation and traction. The traction population varies from >50% to 90%, whereas the saltation population varies from 10% to 40% with a very less proportion of suspension load. The truncation point between traction and saltation lies between -1.5Φ and 0.75Φ while that between saltation and suspension lies between 1.0Φ and 3.5Φ. The

cumulative frequency curves (Fig. 6.9b) for sediments belonging to second cycle also shows two truncation points, one between suspension and saltation and other between saltation and traction. The traction population ranges between 45% and 65%, whereas saltation population varies between 30% and 50%. The truncation point between traction and saltation lies between -1.0Φ and 1.0Φ whereas between saltation and suspension, it lies between 3.0Φ and 3.5Φ. The cumulative frequency curves (Fig. 6.10b) for the sediments belonging to third cycle displays two categories; one with two saltation sub-populations and other with a single saltation population. The traction population ranges between 25% and 85% whereas the saltation population ranges between 12% and 60%. Between traction and saltation, the truncation point lies between 0.5Φ and -1.0Φ however, between saltation and suspension, it lies between 1.0Φ and 2.0Φ. The cumulative frequency curve (Fig. 6.11b) of the sediment belonging to fourth cycle displays two truncation points; one between traction and saltation and the other between saltation and suspension. The traction population constitutes around 85% by weight of the sample whereas saltation load constitutes around 12%, with minor proportion (<3%) of suspension population. The truncation point between traction and saltation lies at 1.0Φ whereas between saltation and suspension, it lies at 3.9Φ.

[III] Bivariant Discriminant Plots –

The bivariant discriminatory plots of Moiola and Weiser (1968), shows that all the sand samples belonging to first, second, third and fourth cycle, falls within the river domain (Fig. 6.3). The scatter plot of Stewart (1958) indicates that these sediments were transported and/or deposited by river process (Fig. 6.4). The Gleister and Nelson (1974) plot displays that all these sediments fall in the intermediate region between alluvial fan and braided bar (Fig. 6.5).

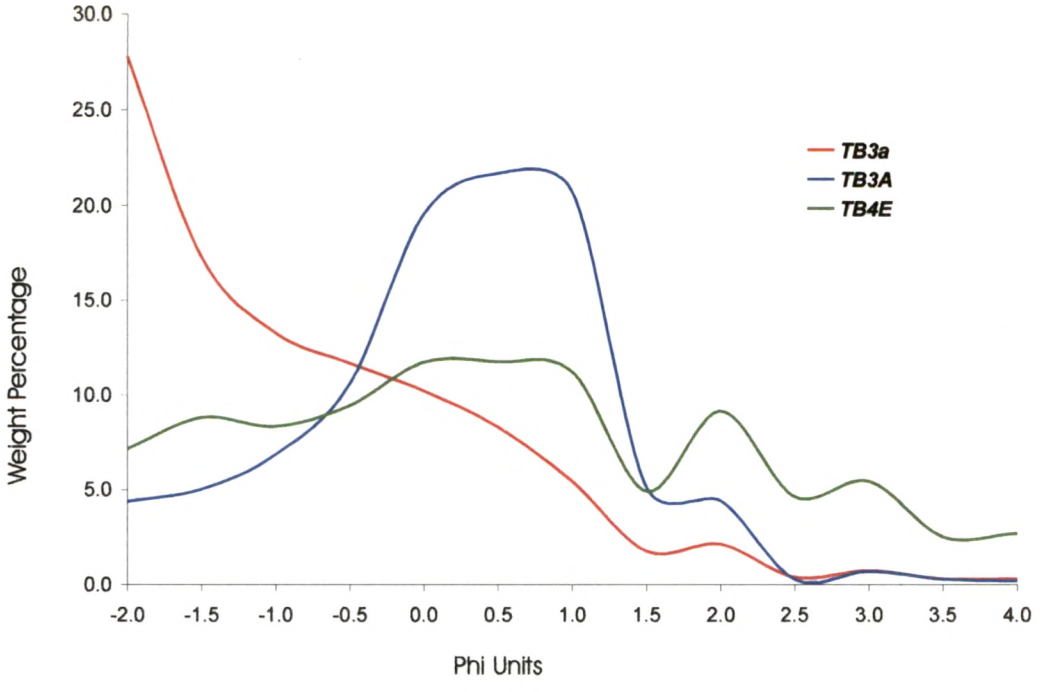

Fig. 6.8a - Diagram Showing The Frequency Curve Of Sediments Belonging To First Cycle Of Quaternary Succession (Loc:- Tapi River).

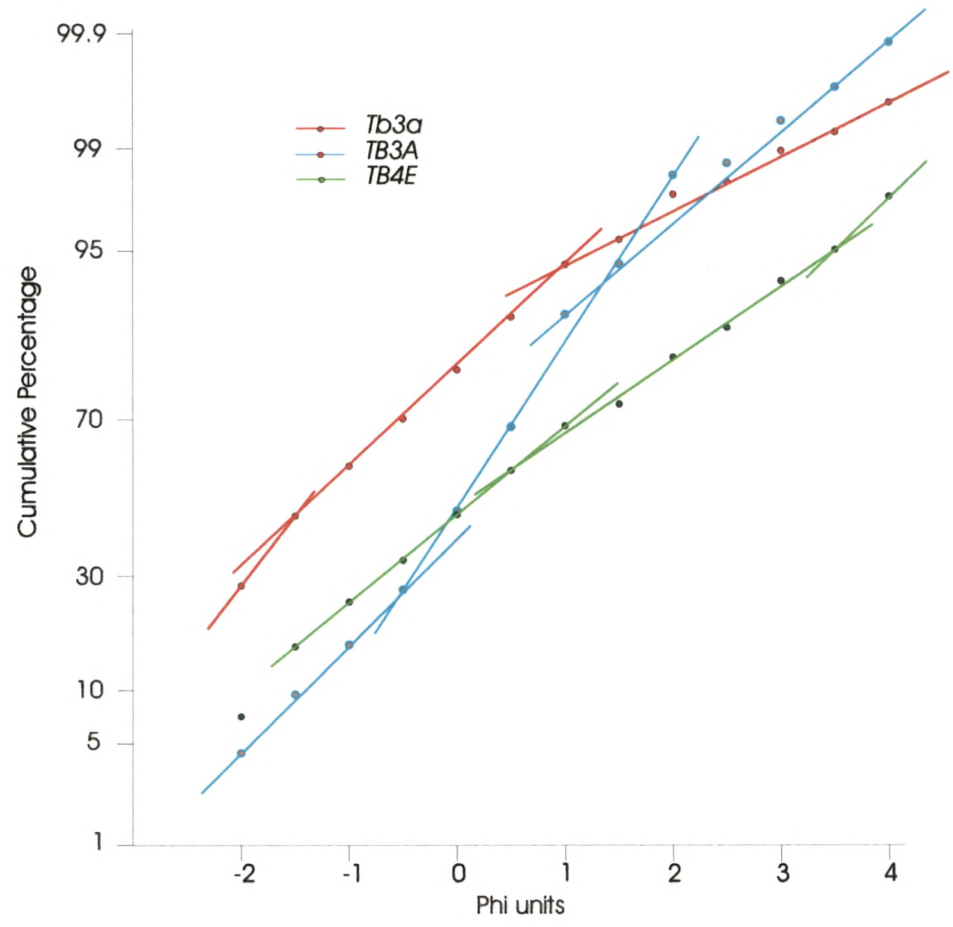

Fig. 6.8b - Diagram Showing The Cumulative Frequency Curve Of Sediments Belonging To First Cycle Of Quaternary Succession (Loc:- Tapi River).

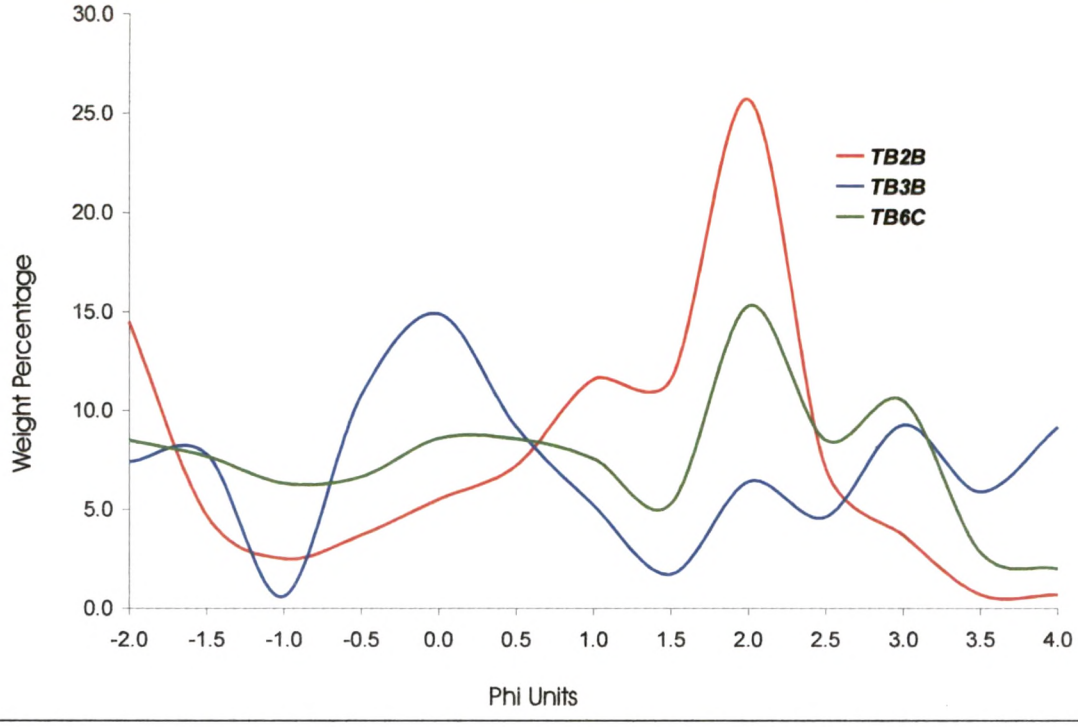

Fig. 6.9a - Diagram Showing The Frequency Curve Of Sediments Belonging To Second Cycle Of Quaternary Succession (Loc:- Tapi River).

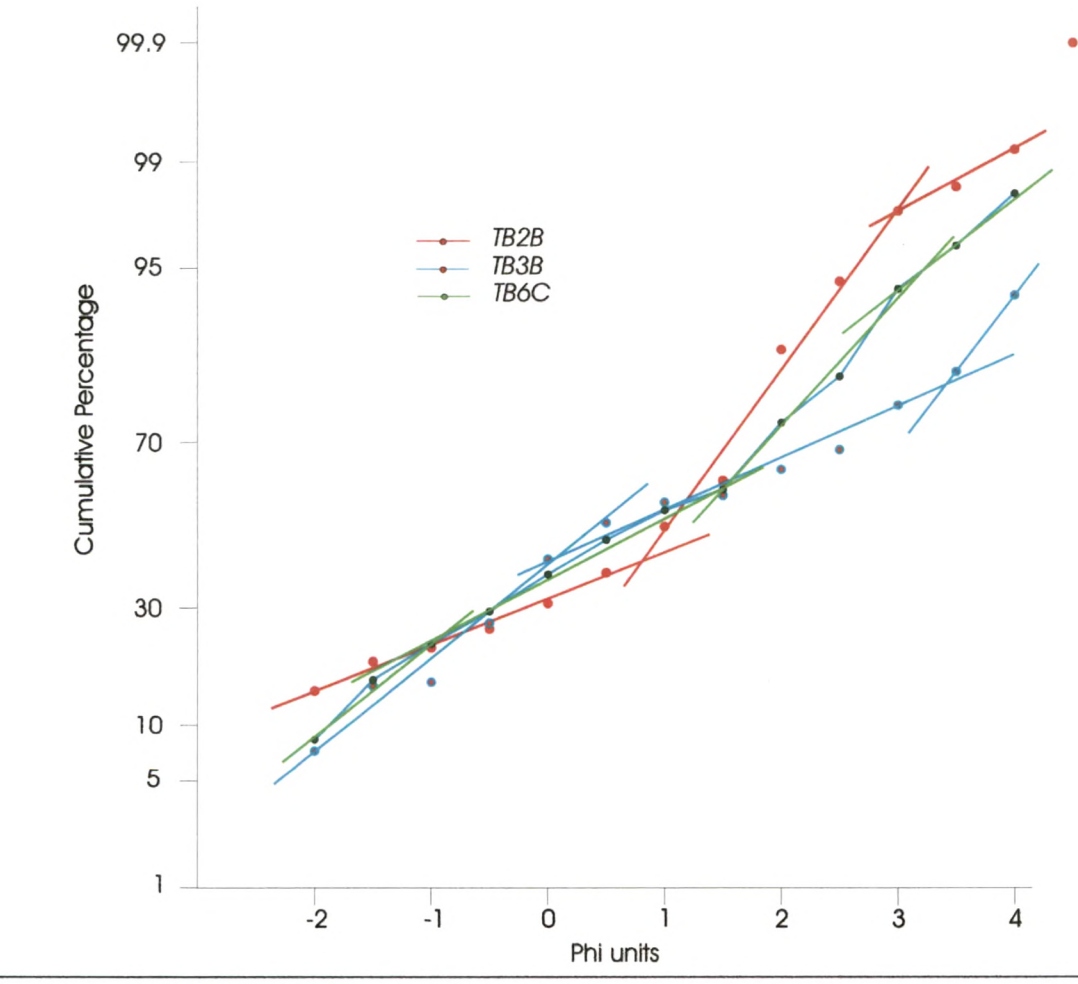

Fig. 6.9b - Diagram Showing The Cumulative Frequency Curve Of Sediments Belonging To Second Cycle Of Quaternary Succession (Loc:- Tapi River).

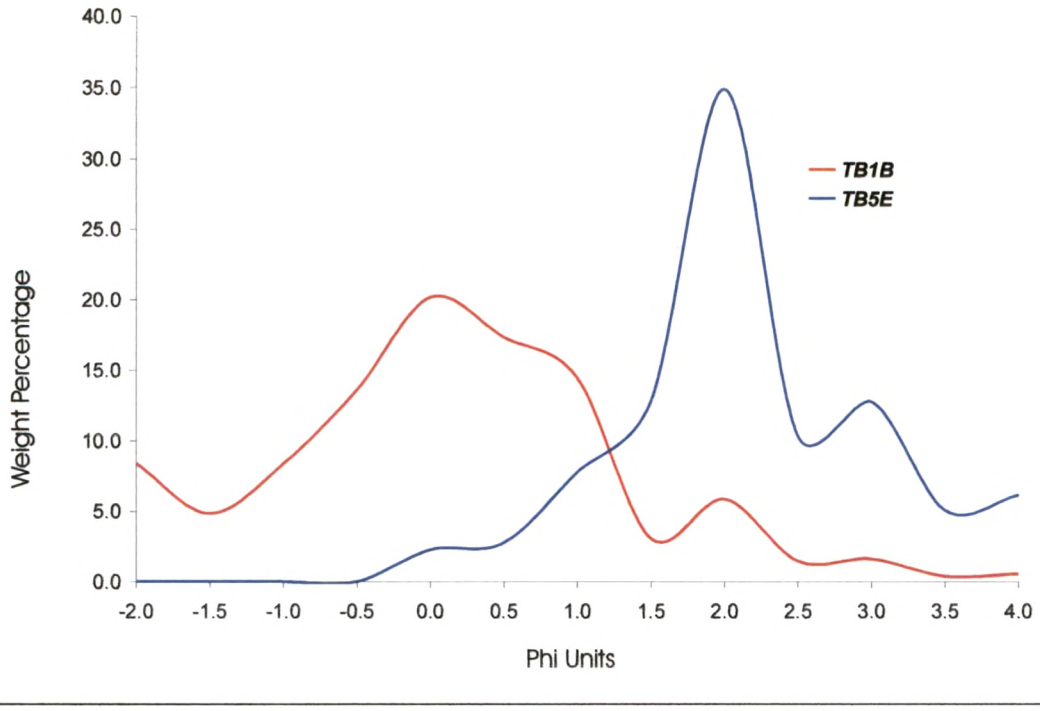

Fig. 6.10a - Diagram Showing The Frequency Curve Of Sediments Belonging To Third Cycle Of Quaternary Succession (Loc:- Tapi River).

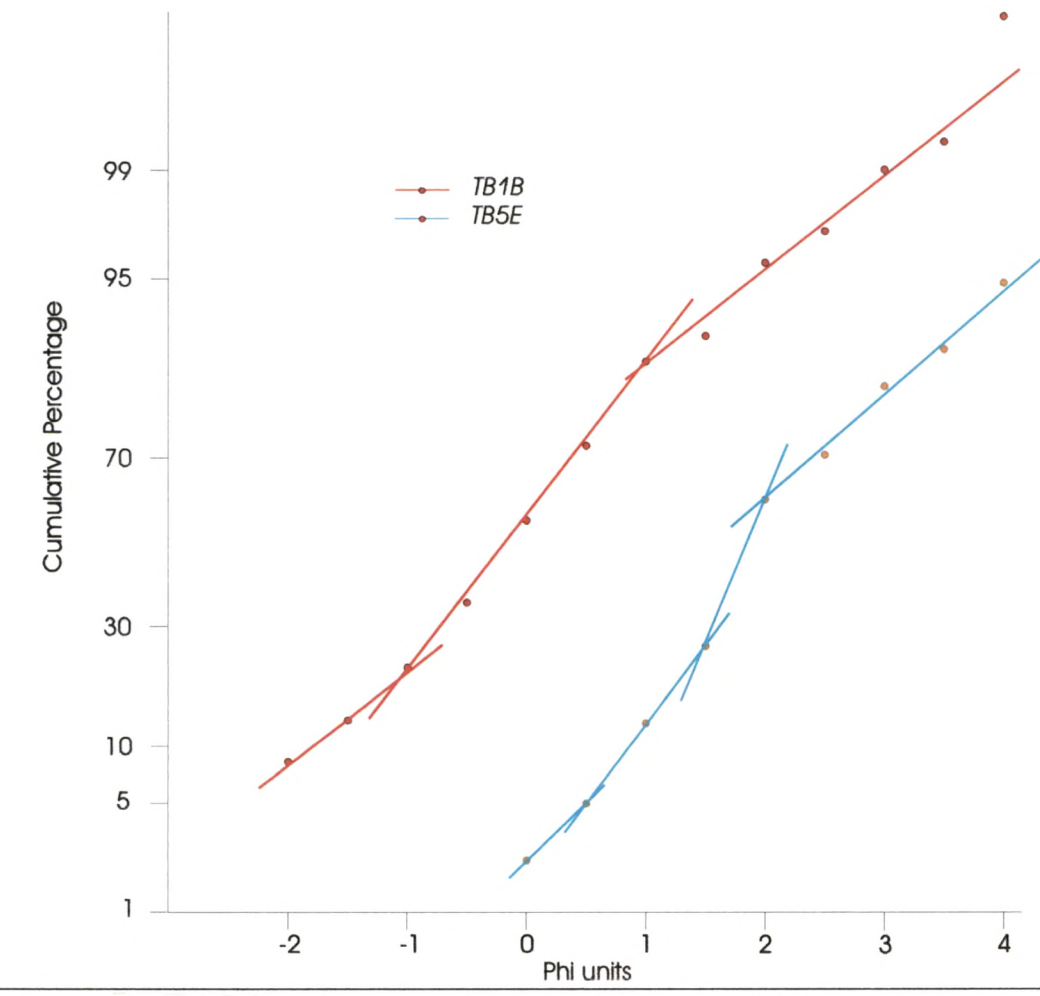

Fig. 6.10b - Diagram Showing The Cumulative Frequency Curve Of Sediments Belonging To Third Cycle Of Quaternary Succession (Loc:- Tapi River).

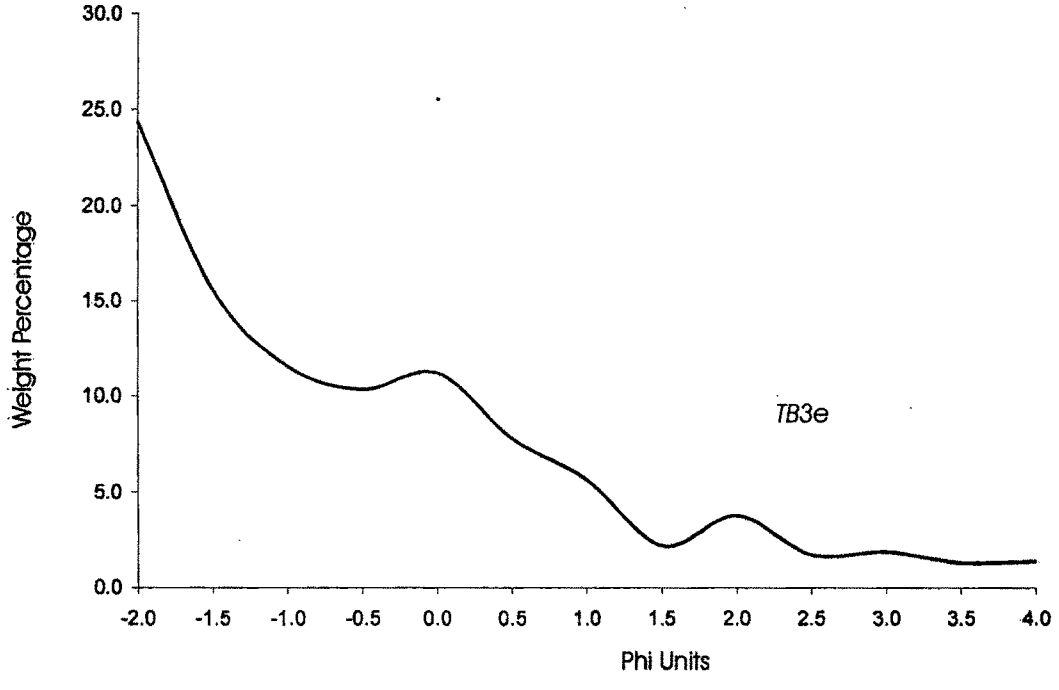

Fig. 6.11a - Diagram Showing The Frequency Curve Of Sediments Belonging To Fourth Cycle Of Quaternary Succession (Loc:- Tapi River).

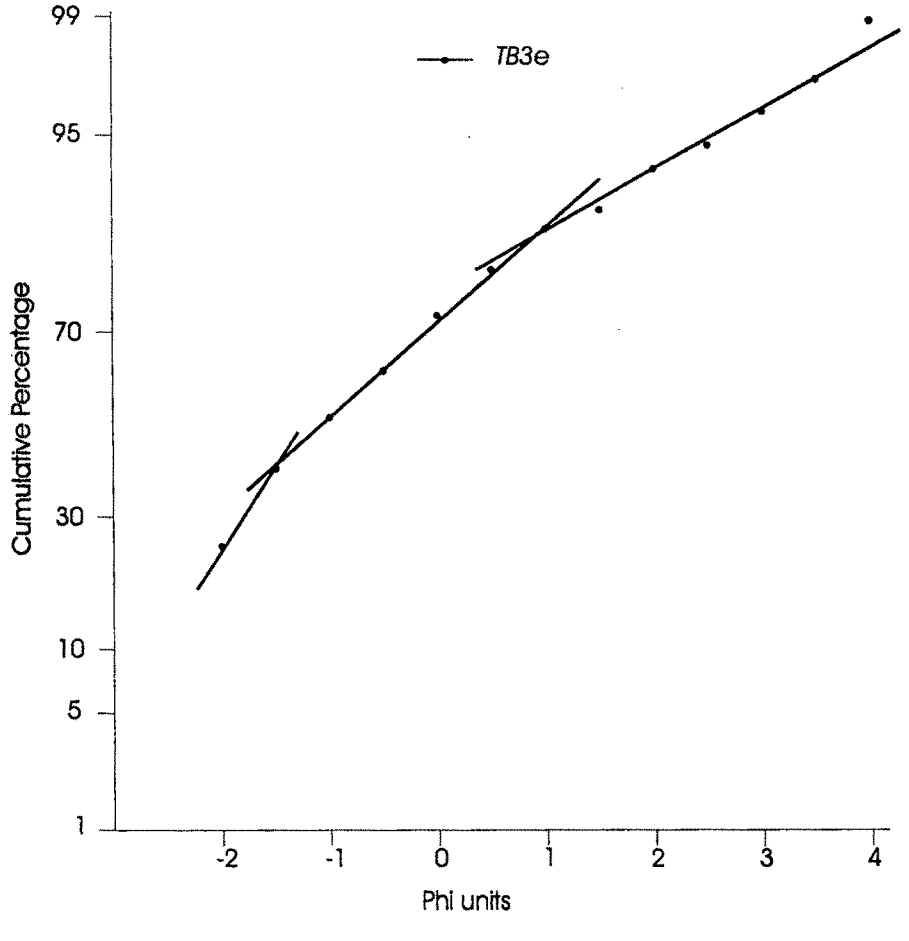

Fig. 6.11b - Diagram Showing The Cumulative Frequency Curve Of Sediments Belonging To Fourth Cycle Of Quaternary Succession (Loc:- Tapi River).

The log – log plot of Sahu (1964) shows that these sediments fall within the fluvial domain (Fig. 6.6).

[IV] C-M Plots –

The C-M diagram plotted for sediments belonging to various cycles of Quaternary successions along the Tapi river (Fig. 6.7), is not completely represented and all the points fall above the ON segment of Passega's standard pattern, except one sample (TB5E), which falls in the PO segment, thereby indicating a probable transportation of this particular sample by means of bottom suspension and strong turbulence, where some rolled grains are also incorporated. All the other samples show a transporting by means of rolling process. It is also observed that the samples show scattering nature, indicating a poor sorting nature of the samples.

6.1.3 Mindhola River

The Quaternary sediment successions encountered at various locations along the Mindhola river, represents four cycles of fining upward sequences. Around 12 samples representing the sand units of these cycles of sedimentation were treated for granulometric analyses, the results of which are provided in the following paragraphs.

[I] Grain Size Parameters –

(a) Graphic Mean (M_Z): The M_Z values obtained for the sediments belonging to second cycle (MB3A, MB6C & MB7B), varies from -2.22Φ to 0.41Φ with an average of -0.87Φ, indicating a very coarse sand size, while those for the sediment belonging to third cycle (MB5J) is 0.17Φ, indicating a coarse sand size. Similarly, the sediments belonging to fourth

cycle (MB3F, MB3G, MB4B, MB4C, MB5E, MB5F, MB7I & MB7J), also represents a coarse sand size with the M_Z values ranging between -2.86Φ to 2.52Φ with an average of 0.60Φ.

(b) Standard Deviation (σ_I): The σ_I values obtained for the sediments belonging to second cycle range from 1.35Φ to 2.09Φ with an average of 1.81Φ, for the sediment belonging to third cycle, it is 1.96Φ and for the sediments belonging to fourth cycle, the values varies between 0.48Φ and 2.50Φ with an average of 1.33Φ. Overall these values indicate that the sediments are poorly sorted in nature.

(c) Inclusive Graphic Skewness (SK_I): The SK_I values for the sediments belonging to second and fourth cycle range between -0.24 and 0.31 (av. 0.02) and between -0.23 and 0.26 (av. -0.07) respectively, indicating a near symmetrical nature however, the SK_I value for the sediment belonging to third cycle is 0.18, indicating a fine-skewed nature of the frequency curve.

(d) Graphic Kurtosis (K_G): The K_G values of the sediments belonging to second and third cycle are 1.00 and 0.98 respectively, thereby indicating a mesokurtic nature, whereas the K_G values of sediment belonging to fourth cycle ranges between 0.95 and 2.01 with an average of 1.35 representing a leptokurtic nature.

[II[Grain Size Distribution Curves –

The grain size frequency distribution curves of the sediments belonging to second and third cycles (Fig. 6.12a, Fig. 6.13a), show a dominance of coarser fragments (-2.0Φ) with minor proportions of pan-fraction (2 – 3%). Majority of the curves representing these sediments, show primary mode at -2.0Φ and the secondary mode between 1.0Φ and 2.0Φ. However, in

one of the samples, MB6C, the primary mode is represented at 1.0Φ. In case of the samples belonging to the fourth cycle (Fig. 6.14a), the sediments show dominance of fine to medium sands and minor proportions of pan-fraction (<2%). The curves representing all these sediments show primary mode at 2.0Φ and secondary mode between 2.5Φ and 3.0Φ; however in case of sample (MB3F), the primary mode is observed at 0.0Φ.

The cumulative frequency size distribution curves for the sediments belonging to second cycle (Fig. 6.12b) show the traction population around 30% to 55% by weight of the sample, whereas saltation population varies from 35% to 50%. The truncation point between traction and saltation lies between -1.5Φ and 0.5Φ however, between saltation and suspension, it lies between 3.5Φ and 4.0Φ. The cumulative frequency curve for the sediment belonging to third cycle shows two truncation points, one between traction and saltation whereas the other between saltation and suspension (Fig. 6.13b). The traction population is around 25% and saltation population is around 72%. The break point between traction and saltation lies at -1.5Φ and that between saltation and suspension lies at 3.5Φ. The cumulative frequency curves for the sediments belonging to fourth cycle display two categories; one having two saltation sub-populations and other with one saltation population (Fig. 6.14b). The traction population for all these samples ranges from 15% to 90%, whereas the saltation population ranges from 12% to 70% with very less proportion of suspension load. The truncation point between traction and saltation lies between -1.5Φ and 1.5Φ while that between saltation and suspension, it lies between 3.5Φ and 4.25Φ.

[III] Bivariant Discriminant Plots –

The bivariant plots of Moiola and Weiser (1968), shows that the sediments belonging to second, third and fourth cycles, fall within the river domain (Fig. 6.3), however, one of the

sample belonging to the fourth cycle (MB3G) falls in the beach domain. The bivariant plot suggested by Stewart (1958) indicates that these sediments have been transported and deposited by river processes (Fig. 6.4); however, the sediment belonging to sample MB3G seems to have transported and deposited by wave processes. The plot (Fig. 6.5) of Gleister and Nelson (1974) clearly indicates that these sediments fall between the domains of alluvial fan and braided bar, however the sediment belonging to fourth cycle falls in the region between alluvial fan and point bar. The log – log plot of Sahu (1964) shows that the sediments representing second and fourth cycles fall in the turbidite domain (Fig. 6.6).

[IV] C-M Plots –

Likewise the C-M diagrams plotted for Kim and Tapi rivers, similar plots for sediments belonging to Mindhola river (Fig. 6.7) is also not completely represented and all the samples fall above the ON segment of Passega's standard pattern, indicating a probable transporting process by rolling of coarser sediments. However, one sample (MB3G) falls in the QR segment, which indicates that this sediment is probably transported as a graded suspension.

6.2 X-RAY DIFFRACTION STUDIES

The X-ray diffraction analyses, which include the bulk as well as clay mineralogical studies, have been carried out for more than 30 samples representing various lithological units of Quaternary successions exposed along the Kim, Tapi and Mindhola rivers, in order to understand the overall mineralogical details.

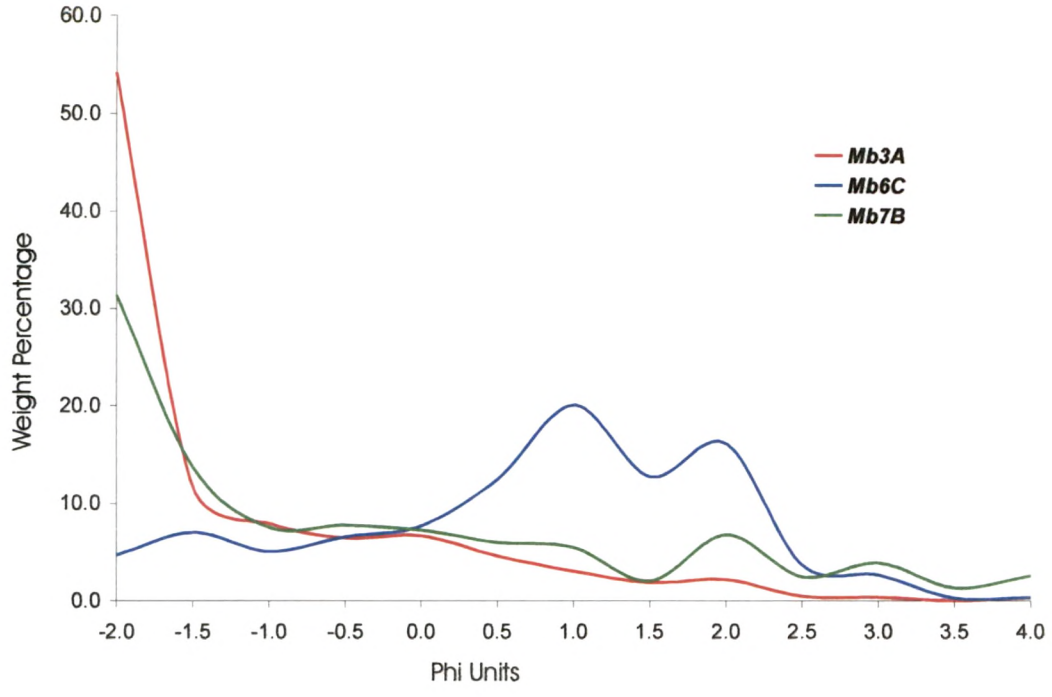

Fig. 6.12a - Diagram Showing The Frequency Curve Of Sediments Belonging To Second Cycle Of Quaternary Succession (Loc:- Mindhola River).

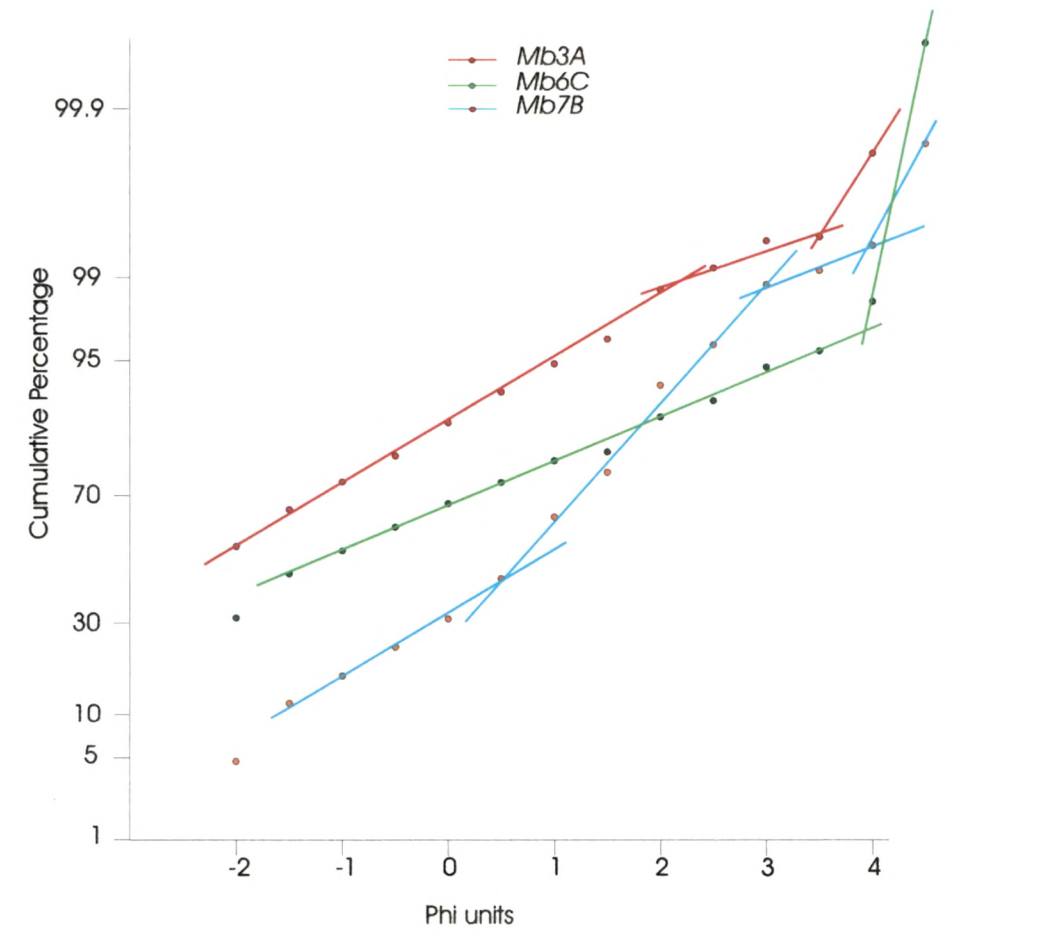

Fig. 6.12b - Diagram Showing The Cumulative Frequency Curve Of Sediments Belonging To Second Cycle Of Quaternary Succession (Loc:- Mindhola River).

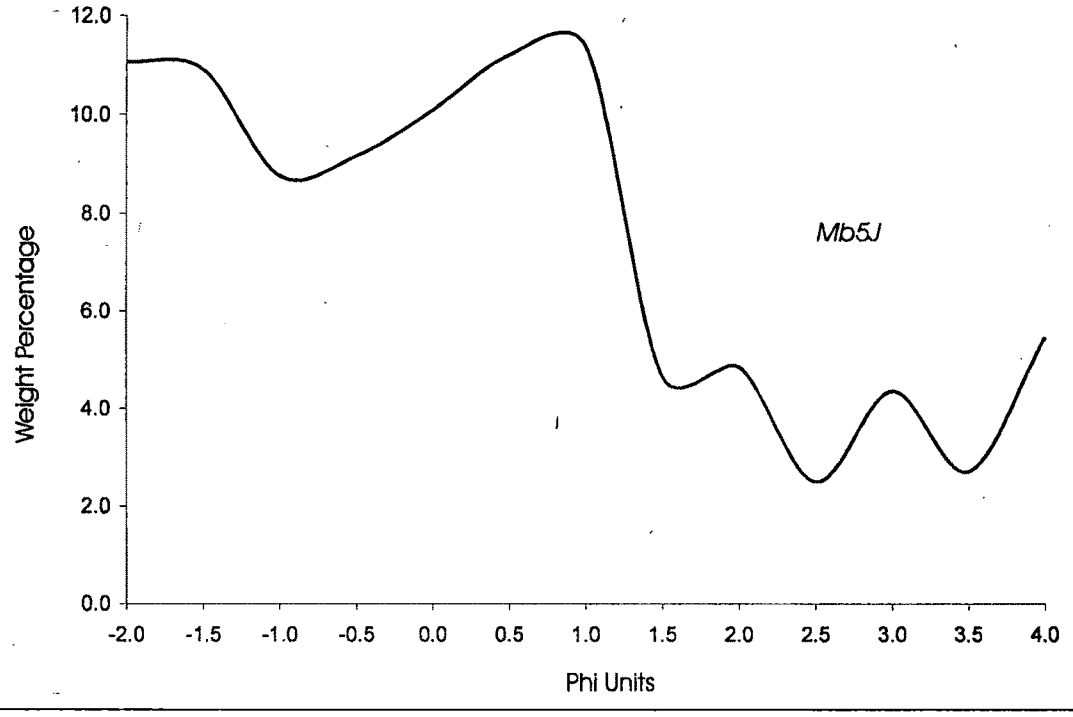

Fig. 6.13a - Diagram Showing The Frequency Curve Of Sediments Belonging To Third Cycle Of Quaternary Succession (Loc:- Mindhola River).

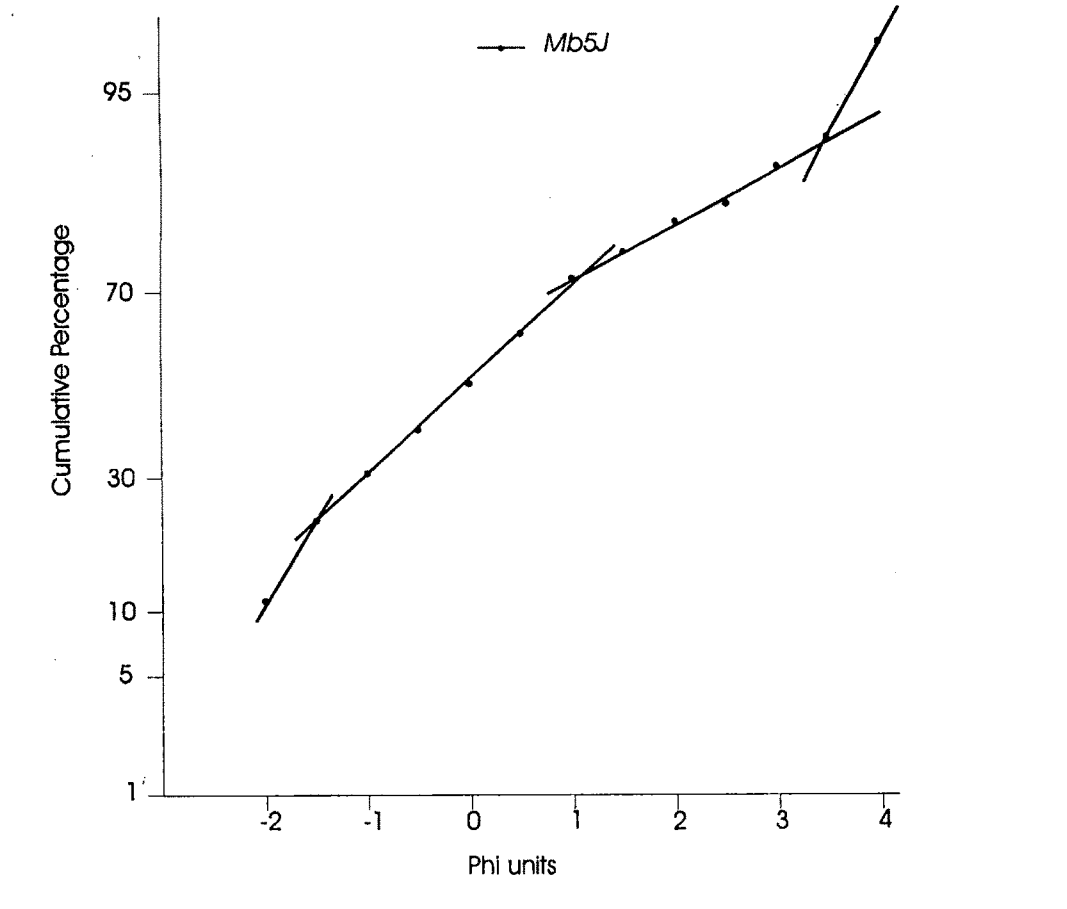

Fig. 6.13b - Diagram Showing The Cumulative Frequency Curve Of Sediments Belonging To Third Cycle Of Quaternary Succession (Loc:- Mindhola River).

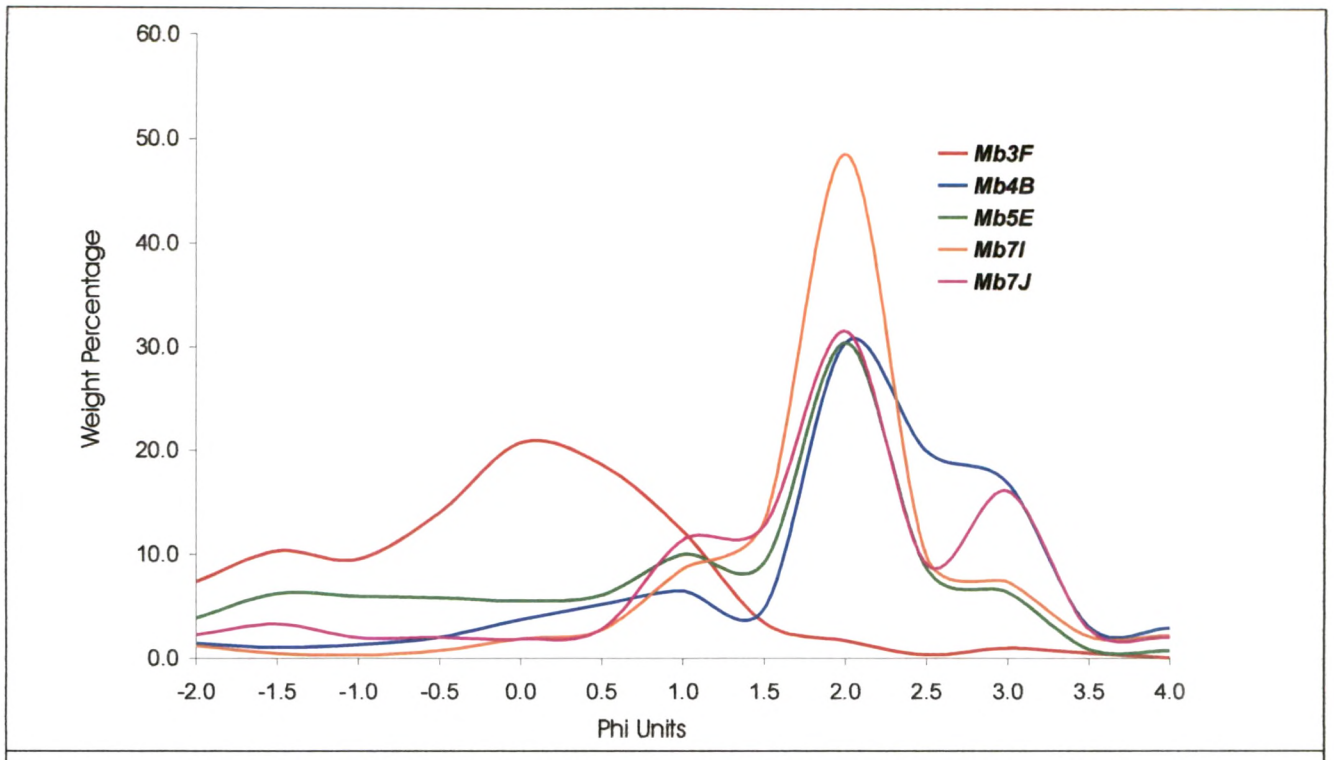

Fig. 6.14a - Diagram Showing The Frequency Curve Of Sediments Belonging To Fourth Cycle Of Quaternary Succession (Loc:- Mindhola River).

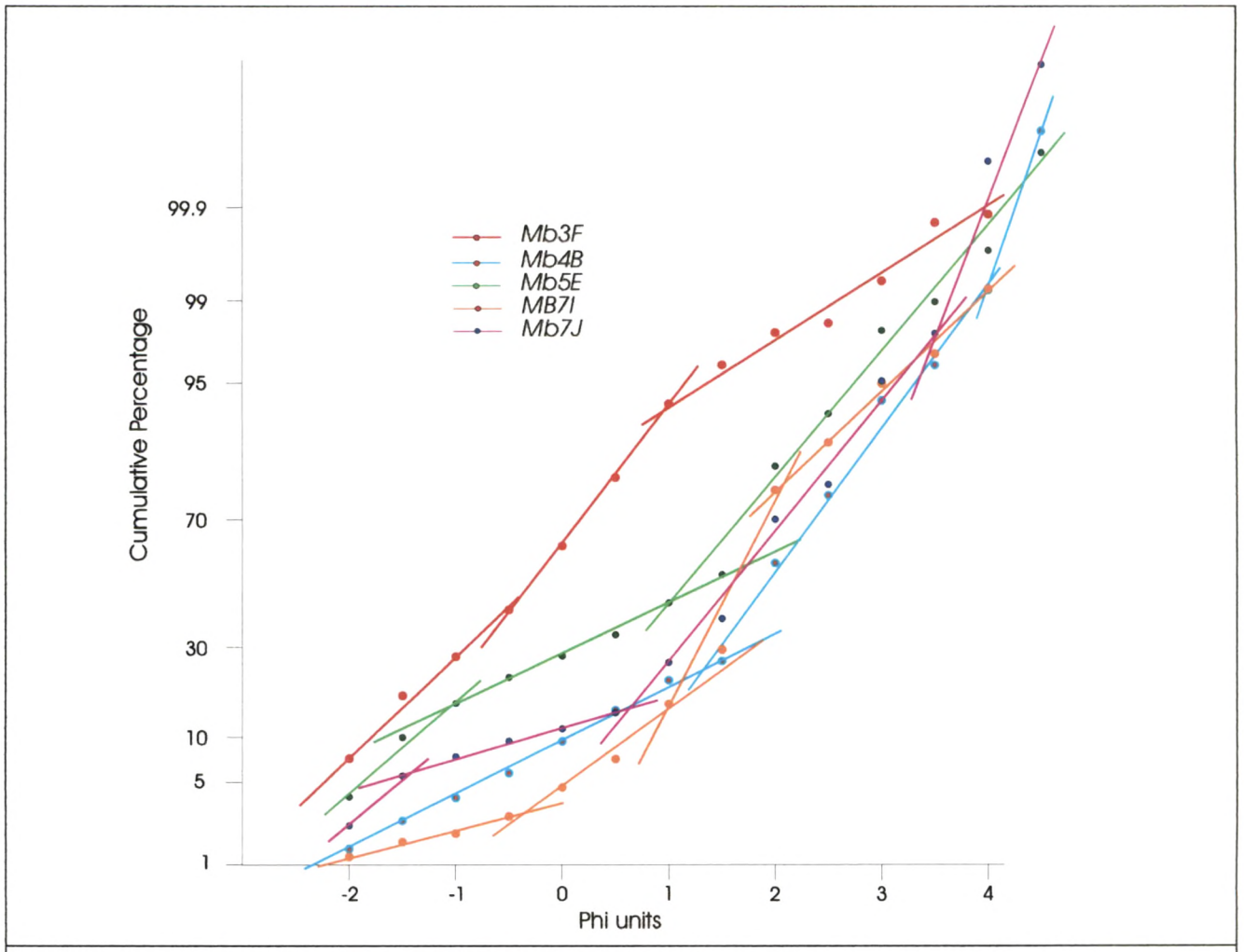

Fig. 6.14b - Diagram Showing The Cumulative Frequency Curve Of Sediments Belonging To Fourth Cycle Of Quaternary Succession (Loc:- Mindhola River).

For bulk mineralogical studies, individual samples were finely powdered by using an agate mortar and were allowed to pass through # 230 ASTM mesh. These samples were then scanned from 3^0 to 45^0 with a scan speed of 0.02^0 2θ/sec and chart speed of 10mm/ ^{0}2θ, using Philips PW 1840 and Rigaku GeigerFlex X-Ray diffractometers, having nickel filtered Cu kα radiation. The diffractograms obtained from these analyses were compared with the standard charts (JCPDS Cards, 1974) of different minerals to obtain the 2θ values, d-spacing and peak intensities and later interpreted adopting the method suggested by Griffin (1971).

The envisaged mineralogical details of the samples belonging to Kim, Tapi and Mindhola river along with their corresponding 2θ values, d-spacing and peak intensities are furnished in table 6.2. Table 6.3 provides the percentage wise assemblages of various minerals identified within the samples under investigation.

Sample No.	*2θ*	*d-spacing*	*Intensity*	*Mineral*
KmB3D	5.64	15.65	100	Smectite
	20.76	4.27	35	Quartz
	26.6	3.35	100	Quartz
	27.9	3.20	100	Plagioclase
	29.36	3.04	100	Calcite
KmB3C	5.52	15.99	100	Smectite
	20.7	4.29	35	Quartz
	26.5	3.36	100	Quartz
	27.7	3.22	100	Plagioclase
KmB1J	20.8	4.27	35	Quartz
	26.7	3.34	100	Quartz
	28.0	3.20	100	Plagioclase
	29.6	3.02	100	Calcite
KmB1F	5.8	15.24	100	Smectite
	20.8	4.27	35	Quartz
	26.7	3.34	100	Quartz
	27.8	3.21	100	Plagioclase
	29.0	3.08	100	Calcite
KmB1D	20.8	4.27	35	Quartz
	26.7	3.34	100	Quartz
	28.0	3.20	100	Plagioclase
	29.6	3.02	100	Calcite
	43.3	2.09	18	Calcite
KmB1C	5.8	15.24	100	Smectite
	20.8	4.27	35	Quartz
	26.7	3.34	100	Quartz
	28.0	3.19	100	Plagioclase
	29.4	3.04	100	Calcite

KmB4B	5.02	17.5	100	Smectite
	5.96	14.82	100	Chlorite
	20.66	4.295	35	Quartz
	26.5	3.35	100	Quartz
	27.8	3.21	100	Plagioclase
	29.3	3.04	100	Calcite
	39.3	2.29	12	Quartz
KmB4A	5.66	15.6	100	Smectite
	6.18	14.29	100	Chlorite
	20.76	4.275	35	Quartz
	26.5	3.35	100	Quartz
KmB1B	20.8	4.27	35	Quartz
	26.7	3.34	100	Quartz
	28.0	3.20	100	Plagioclase
	29.6	3.02	100	Calcite
TB3E	20.8	4.27	35	Quartz
	22.0	4.04	16	Plagioclase
	26.5	3.36	100	Quartz
	28.0	3.19	100	Plagioclase
	29.6	3.02	100	Calcite
	35.6	2.52	40	Biotite
	36.6	2.45	12	Quartz
TB3e	20.8	4.27	35	Quartz
	22.1	4.02	16	Plagioclase
	26.8	3.33	100	Quartz
	28.0	3.19	100	Plagioclase
	29.6	3.02	100	Calcite
	36.7	2.45	12	Quartz
TB4K	5.8	15.24	100	Smectite
	20.8	4.27	35	Quartz
	21.8	4.08	16	Plagioclase
	26.5	3.36	100	Quartz
	27.8	3.21	100	Plagioclase
	29.4	3.04	100	Calcite
TB4J	5.68	15.54	100	Smectite
	6.72	13.14	100	Chlorite
	20.8	4.27	35	Quartz
	26.5	3.36	100	Quartz
	27.8	3.21	100	Plagioclase
	29.4	3.04	100	Calcite
TB3D	20.8	4.27	35	Quartz
	26.7	3.34	100	Quartz
	27.8	3.21	100	Plagioclase
	29.5	3.03	100	Calcite
	43.4	2.09	18	Calcite
TB4I	5.9	14.87	100	Smectite
	26.5	3.36	100	Quartz
	27.9	3.19	100	Plagioclase
	29.4	3.04	100	Calcite
TB4H	5.9	14.87	100	Smectite
	26.6	3.35	100	Quartz
	27.6	3.22	100	Plagioclase
	29.4	3.04	100	Calcite
TB3B	20.8	4.27	35	Quartz
	26.7	3.34	100	Quartz

	28.0	3.19	100	Plagioclase
	29.5	3.03	100	Calcite
	43.4	2.08	18	Calcite
TB4B	20.8	4.27	35	Quartz
	26.7	3.34	100	Quartz
	27.8	3.21	100	Plagioclase
	29.4	3.04	100	Calcite
	34.7	2.58	40	Biotite
	43.3	2.09	18	Calcite
TB3b	20.8	4.27	35	Quartz
	22.0	4.04	16	Plagioclase
	26.7	3.34	100	Quartz
	28.0	3.19	100	Plagioclase
	29.5	3.03	100	Calcite
TB3A	5.8	15.24	100	Smectite
	23.7	3.75	100	Orthoclase
	26.7	3.34	100	Quartz
	27.9	3.20	100	Plagioclase
	29.7	3.02	100	Calcite
MB5E	5.8	15.24	100	Smectite
	20.7	4.29	35	Quartz
	22.0	4.04	16	Plagioclase
	26.7	3.34	100	Quartz
	27.8	3.21	100	Plagioclase
	29.7	3.03	100	Calcite
MB5D	5.5	16.07	100	Smectite
	20.7	4.29	35	Quartz
	26.5	3.36	100	Quartz
	27.5	3.24	90	Orthoclase
	27.8	3.21	100	Plagioclase
	29.6	3.02	100	Calcite
MB5C	5.8	15.24	100	Smectite
	20.8	4.27	35	Quartz
	21.8	4.08	16	Plagioclase
	26.6	3.35	100	Quartz
	27.8	3.21	100	Plagioclase
	29.6	3.02	100	Calcite
MB5I	5.8	15.24	100	Smectite
	20.9	4.29	35	Quartz
	22.0	4.04	16	Plagioclase
	26.7	3.34	100	Quartz
	27.5	3.24	90	Orthoclase
	27.8	3.21	100	Plagioclase
	29.5	3.03	100	Calcite
MB5G	20.8	4.27	35	Quartz
	26.7	3.34	100	Quartz
	27.4	3.25	90	Orthoclase
	28.2	3.16	100	Plagioclase
	29.5	3.03	100	Calcite
	43.3	2.09	18	Calcite
MB1E	5.7	15.60	100	Smectite
	20.8	4.27	35	Quartz
	26.5	3.36	100	Quartz
	27.4	3.25	90	Orthoclase
	27.9	3.19	100	Plagioclase

	29.3	3.04	100	Calcite
MB1D	6.08	14.52	100	Smectite
	20.8	4.27	35	Quartz
	26.6	3.35	100	Quartz
	27.9	3.19	100	Plagioclase
	29.4	3.03	100	Calcite
MB1C	5.8	15.17	100	Smectite
	20.74	4.28	35	Quartz
	26.5	3.36	100	Quartz
	27.8	3.21	100	Plagioclase
	29.2	3.05	100	Calcite
MB1A	5.5	16.05	100	Smectite
	6.06	14.6	100	Chlorite
	20.78	4.27	35	Quartz
	26.6	3.35	100	Quartz
	27.9	3.20	100	Plagioclase
	29.3	3.04	100	Calcite
MB6B	20.8	4.27	35	Quartz
	26.8	3.33	100	Quartz
	28.0	3.19	100	Plagioclase
	29.6	3.02	100	Calcite

Table 6.2 – Mineralogical Details Of The Quaternary Samples Of The Study Area.

6.2.1 Bulk Mineralogy –

The X-ray diffraction studies of Quaternary sediments along the Kim river show the abundance of minerals such as quartz, plagioclase feldspar and calcite (Fig. 6.15). In addition to these minerals, other minerals such as orthoclase, cristobalite, biotite, epidote, pyroxenes, olivine and goethite have been recorded in minor amounts. The only clay mineral identified in these samples is smectite.

In the case of Quaternary sediments belonging to Tapi river, the X-ray diffraction studies show the dominance of minerals such as quartz, plagioclase feldspar and calcite (Fig. 6.16). Along with these minerals, minor proportions of other minerals such as orthoclase, cristobalite, biotite, epidote, pyroxenes, olivine and goethite have also been recorded. The clay minerals include smectite, illite, chlorite and kaolinite.

Like in the case of Kim and Tapi rivers, the X-ray diffraction studies of the Quaternary sediments, along the Mindhola river, also shows the abundance of minerals such as quartz,

plagioclase feldspar and calcite (Fig. 6.17). In addition to these minerals, presence of other minerals such as cristobalite, biotite, pyroxenes, olivine and goethite have also been deciphered. The clay minerals include smectite, illite, chlorite and kaolinite.

The semi-quantitative analyses have provided some interesting results (Table 6.3). The diffractograms of the sediments representing the Kim river sections show a slight decrease in the proportion of quartz in the upper horizons, whereas calcite is seen occurring in higher abundances in the middle horizons of the stratigraphic succession. The diffractograms of the sediments belonging to Tapi river sections indicate that the proportion of quartz mineral increases from the bottom to the top of the stratigraphic succession, whereas the proportion of calcite decreases. Unlike in case of Tapi river sediments, the diffractograms of the sediments belonging to the Mindhola river sections reflect that the proportion of quartz decreases considerably in the upper horizons of the stratigraphic succession, wherein minerals such as orthoclase and epidote show comparatively higher abundances. The proportions of calcite first decreases and then show an increase in proportion towards the top of the stratigraphic succession.

6.2.2 Clay Mineralogy –

The X-ray diffraction studies for the identification of clay minerals were carried out for the representative sample of clayey sediments obtained from the Quaternary successions exposed along the Kim, Tapi and Mindhola rivers. For clay mineralogical studies about 21 representative samples were processed following the standard procedures suggested by Gibbs (1965) and Caroll (1970).

The samples were scanned from 3^0 to 21^0 with a scan speed of 1^0 2θ/min using Philips PW 1840 X-Ray diffractometer, having nickel filtered Cu kα radiation. The diffractograms obtained from the above studies are represented in figure 6.18.

The clay mineralogical studies of the Quaternary sediments belonging to the Kim, Tapi and Mindhola rivers have shown the overall presence of clay minerals such as smectite, illite, chlorite and kaolinite.

Sample No.	Minerals in %												
	Q	P	Or	Calc	Go	Cr	Ep	B	P(m)	P(o)	O(Fe)	O(Mg)	Total
KmB3D	39.2	8.7	5.2	5.0	5.0	5.9	5.5	5.9	8.9	5.9	4.8	-	100
KmB3C	49.9	6.3	6.6	4.3	5.7	5.7	5.7	-	5.4	6.0	4.3	-	100
KmB1J	42.5	19.3	4.6	14.2	-	3.2	4.9	6.4	-	-	4.9	-	100
KmB1F	40.7	16.5	9.5	22.1	-	3.0	-	-	3.7	-	4.4	-	100
KmB1D	9.9	3.7	31.4	-	6.2	5.4	6.4	-	-	-	-	-	100
KmB1C	35.0	9.7	-	25.8	-	3.1	-	-	6.3	4.7	7.3	8.1	100
KmB4B	37.5	12.8	5.0	7.8	6.3	5.9	-	6.9	5.4	5.4	-	6.9	100
KmB4A	58.4	5.7	6.4	5.7	6.8	5.1	5.4	-	6.4	-	-	-	100
KmB1B	44.1	16.8	-	14.1	-	10.3	7.1	7.6	-	-	-	-	100
TB3E	21.5	19.2	15.2	9.4	-	4.1	10.0	7.0	4.9	3.0	5.7	-	100
TB3e	34.3	20.7	5.5	12.4	-	5.0	8.8	6.6	-	-	6.6	-	100
TB4K	30.0	16.6	6.5	15.5	-	5.7	7.3	6.1	6.5	-	5.9	-	100
TB4J	36.8	19.9	4.9	4.0	4.4	14.4	3.2	4.4	3.4	-	4.7	-	100
TB3D	43.5	16.9	10.4	16.1	-	6.5	-	-	-	4.2	2.3	-	100
TB4I	24.5	9.7	8.2	26.6	8.2	4.8	-	6.5	5.4	-	6.1	-	100
TB4H	41.8	9.4	4.8	12.7	4.1	5.3	6.0	5.8	4.6	5.5	-	-	100
TB3B	23.4	13.2	-	31.5	-	-	-	12.7	7.4	-	6.3	5.6	100
TB4B	28.1	4.7	8.0	34.1	-	-	3.5	6.4	-	1.6	13.7	-	100
TB3b	32.7	10.2	5.7	36.3	-	9.3	2.0	-	-	-	3.8	-	100
TB3A	12.4	45.9	10.0	7.7	-	6.2	6.6	-	-	-	11.2	-	100
MB5E	24.9	11.8	15.2	31.1	-	3.9	4.9	-	8.2	-	-	-	100
MB5D	24.6	13.0	13.0	11.8	-	-	13.0	14.7	9.8	-	-	-	100
MB5C	17.5	20.6	5.4	10.1	-	8.2	28.8	-	9.3	-	-	-	100
MB5I	34.5	13.4	19.5	8.2	-	2.6	7.0	-	11.3	3.5	-	-	100
MB5G	29.4	21.4	22.1	14.1	-	4.6	3.7	-	-	-	4.6	-	100
MB1E	45.3	10.2	6.3	9.9	4.7	5.5	4.9	4.2	-	4.4	4.7	-	100
MB1D	43.6	7.8	3.8	5.3	5.8	13.6	4.0	5.0	4.5	3.3	3.3	-	100
MB1C	57.6	10.6	-	4.3	5.3	4.3	7.6	-	4.0	3.0	3.3	-	100
MB1A	43.6	8.0	6.3	4.5	3.5	4.3	17.5	5.0	3.5	3.8	-	-	100
MB6B	37.0	16.0	7.8	18.9	-	4.0	16.3	-	-	-	-	-	100

Table 6.3 – Semi-Quantitative Analyses Of The Quaternary Sediments Of The Study Area.
{where, Q-Quartz, P-Plagioclase, Or-Orthoclase, Calc-Calcite, Go-Goethite, Cr-Cristobalite, Ep-Epidote, B-Biotite, P(m)- Monoclinal Pyroxene, P(o)- Orthorhombic Pyroxene, O(Fe)-Fe Olivine O(Mg)-Mg Olivine}.

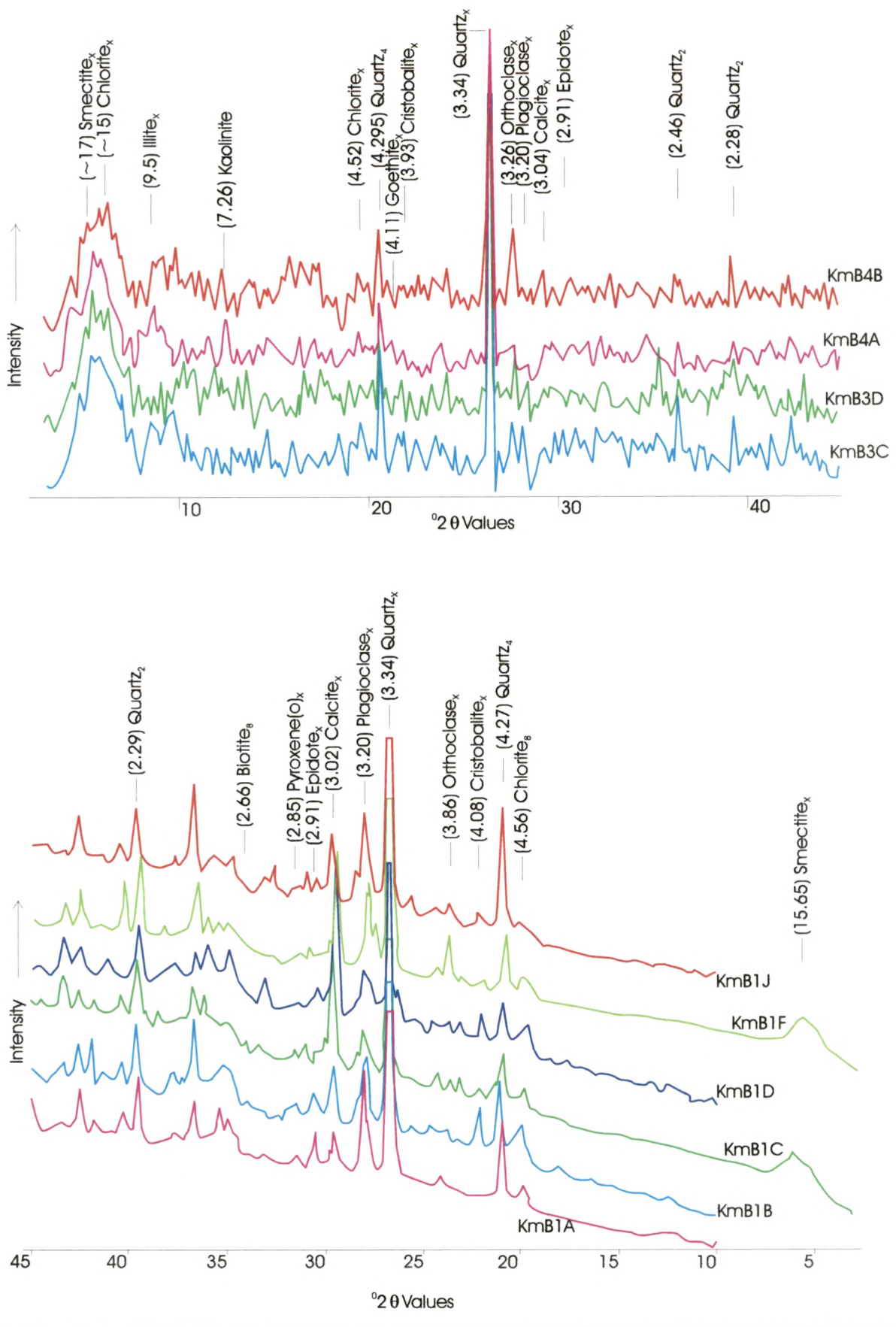

Fig. 6.15 - X-Ray Diffractograms Of Quaternary Sediments Belonging To Kim River.

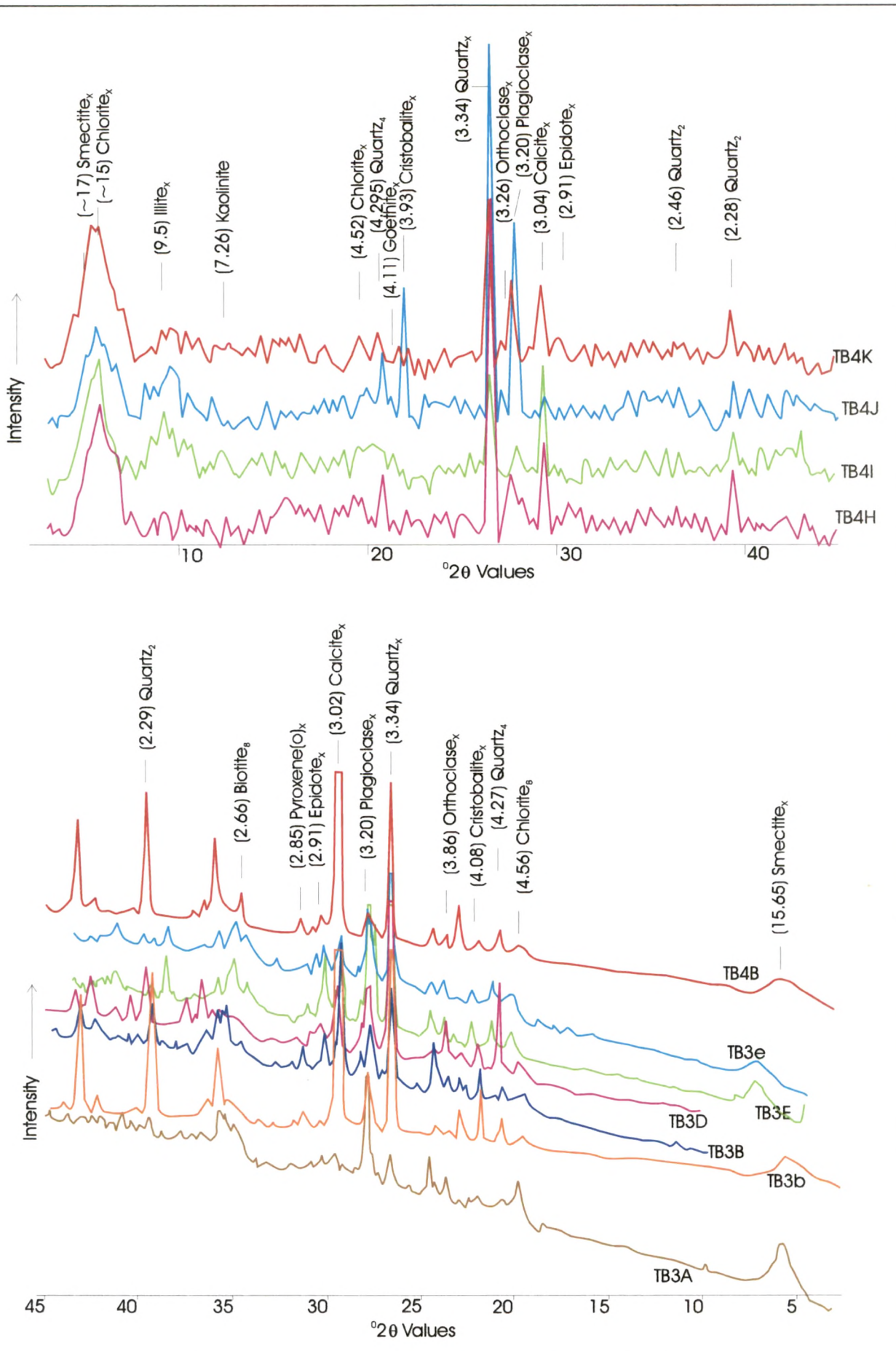

Fig. 6.16 - X-Ray Diffractograms Of Quaternary Sediments Belonging To Tapi River.

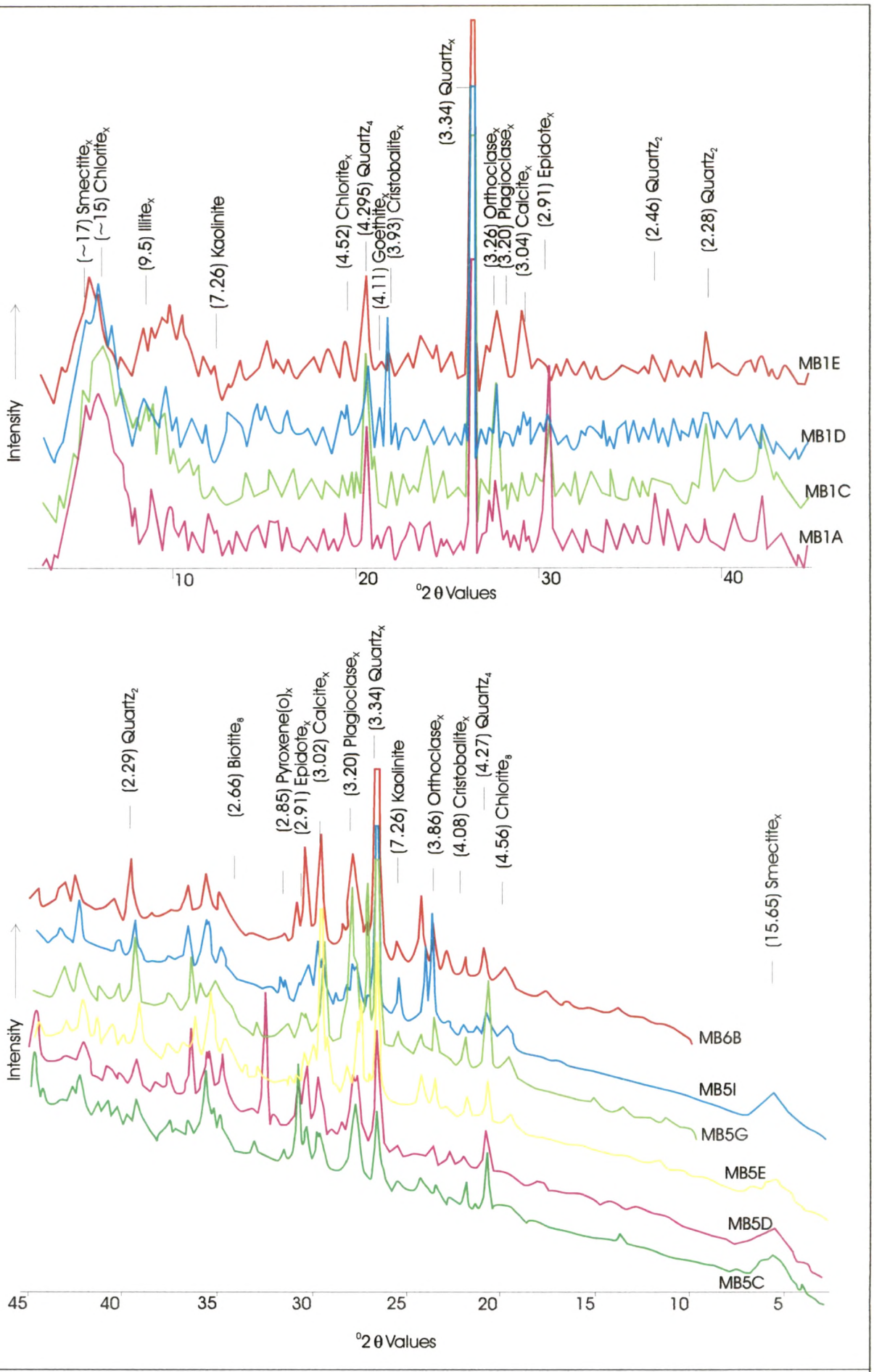

Fig. 6.17 - X-Ray Diffractograms Of Quaternary Sediments Belonging To Mindhola River.

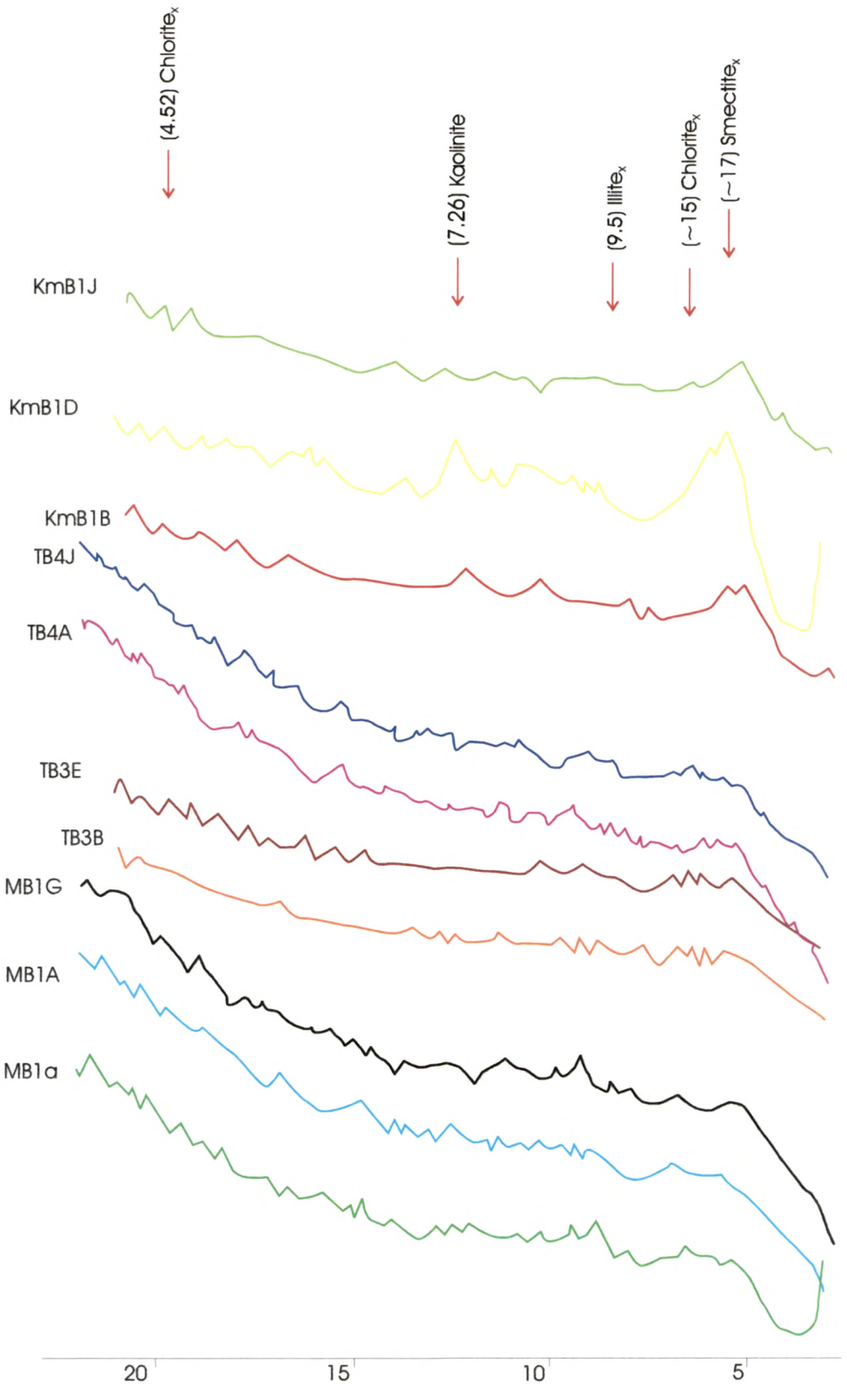

Fig. 6.18 - X-Ray Diffractogram Peaks Of Clay Minerals In Quaternary Sediments Of Study Area.

6.3 SURFACE MORPHOLOGICAL STUDIES

The surface textures of sand grains are examined by using the standard techniques of Scanning Electron Microscopy (SEM). Earlier workers (Krinsley & Donahue, 1968; Krinsley & Doornkamp, 1973; Ly, 1978; Manker & Ponder, 1978; Higgs, 1979; Culver et al., 1983; Manickam & Barbaroux, 1987) have attempted this technique to study the surface textures of quartz grains to understand their transportational history and environment of deposition.

In the present investigation, an attempt has been made to study the surface textures of about 100 grains of quartz representing the sand units exposed within the Quaternary successions distributed throughout the study area, which have been identified and interpreted using the standard references of Krinsley & Doornkamp (1973), Manker & Ponder (1978), Higgs (1979) and Manickam & Barbaroux (1987).

In order to carry out the above studies, the quartz grains were selected from each of the sand members and were treated following the technique suggested by Krinsley & Doornkamp (1973) and Manker & Ponder (1978).

The silt and clay fractions (<62μm) were removed by means of wet sieving. The coarse fragments (>62μm) were dry-sieved and quartz grains of approximately same size and shape were picked up from each of the samples using a binocular microscope. These grains were then treated with dilute hydrogen peroxide (H_2O_2) to remove organic and inorganic matters and finally they were slowly attacked with dilute hydrochloric acid (HCl) to remove coatings. The prepared quartz grains were coated with gold by POLARON – SC502 – Sputter Coater and scanned with a LEO (Leica Electron Optics) Electron Microscopy 430 at various magnifications. Table 6.4 provides a detail account of the surface features observed, which are clearly depicted in figure 6.19, 6.20 & 6.21.

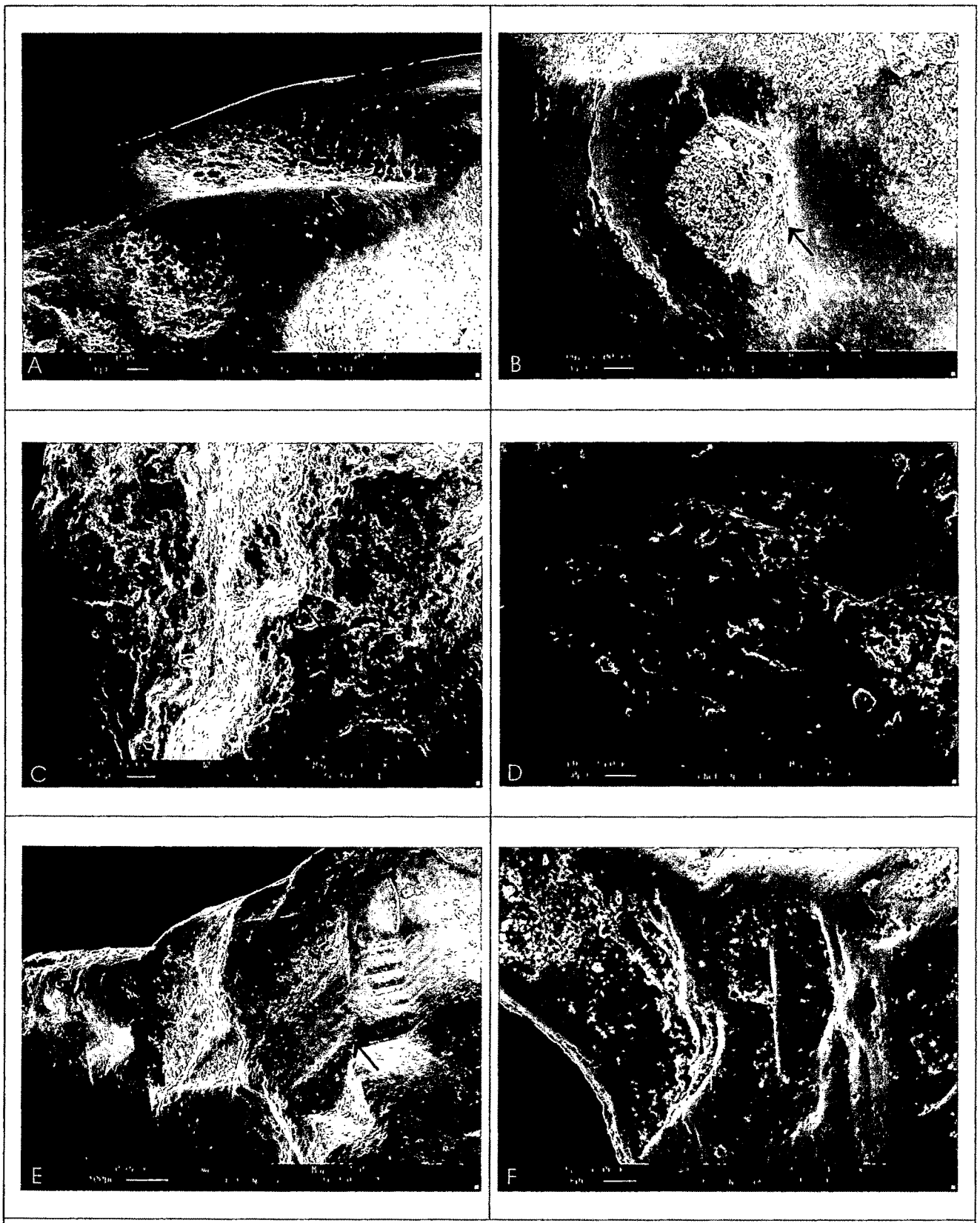

Fig. 6.19 - SEM Photomicrographs Showing The Surface Features Of Quartz Grains (Location - Kim River Sections) [A,B - Impact Features, C - Straight and Curved Steps, D - Straight Scratches, E - Straight Steps and F - Conchoidal Fractures and Mechanically Formed "V"s].

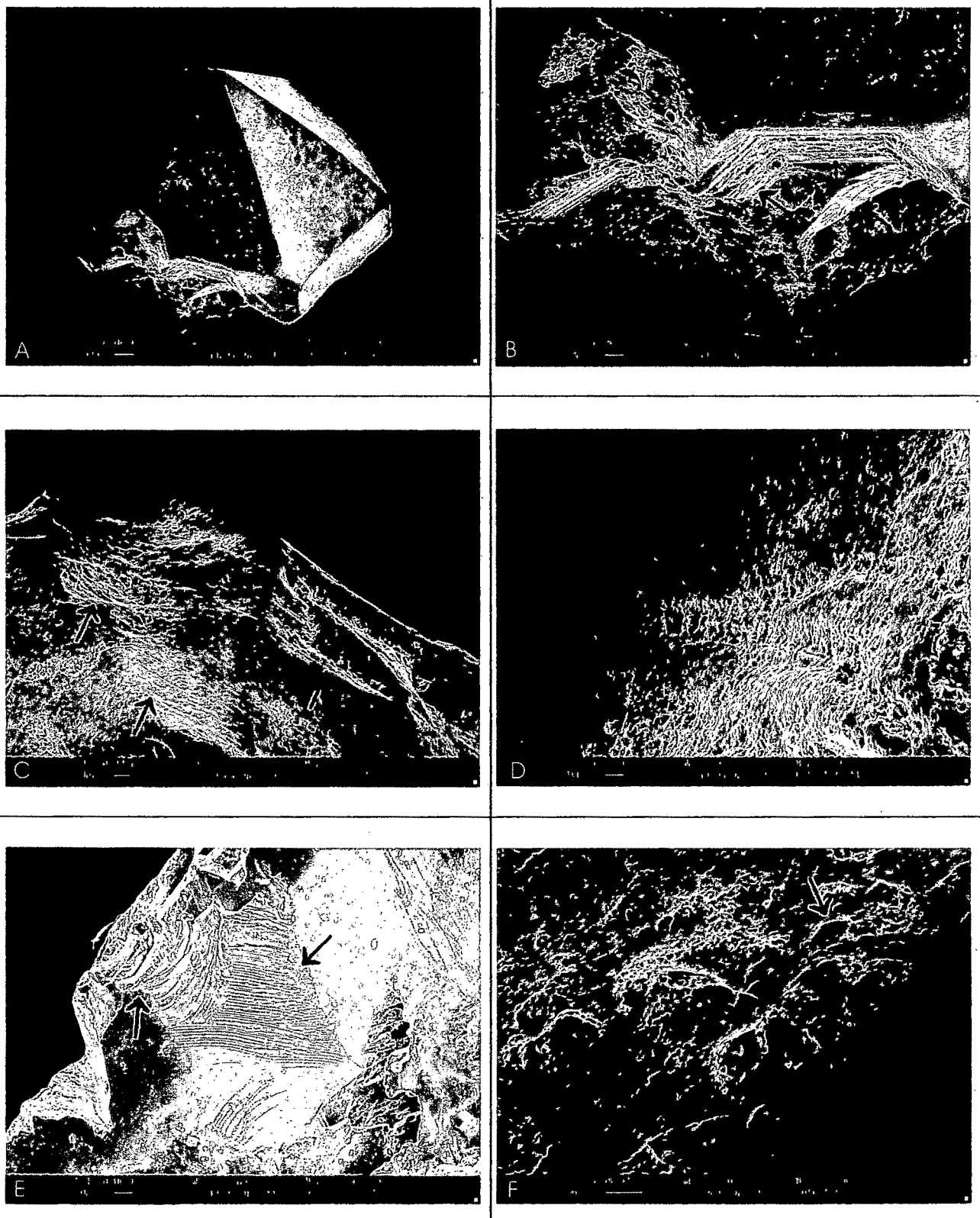

Fig. 6.20 - SEM Photomicrographs Showing The Surface Features Of Quartz Grains (Location - Tapi River Sections) [A - Sub-angular Nature, B,C - Straight and Curved Steps along with Oriented Fractures, D - Impact Features and Straight Scratches, E - Conchoidal Fractures and Straight Steps and F - Mechanically Formed "V"s].

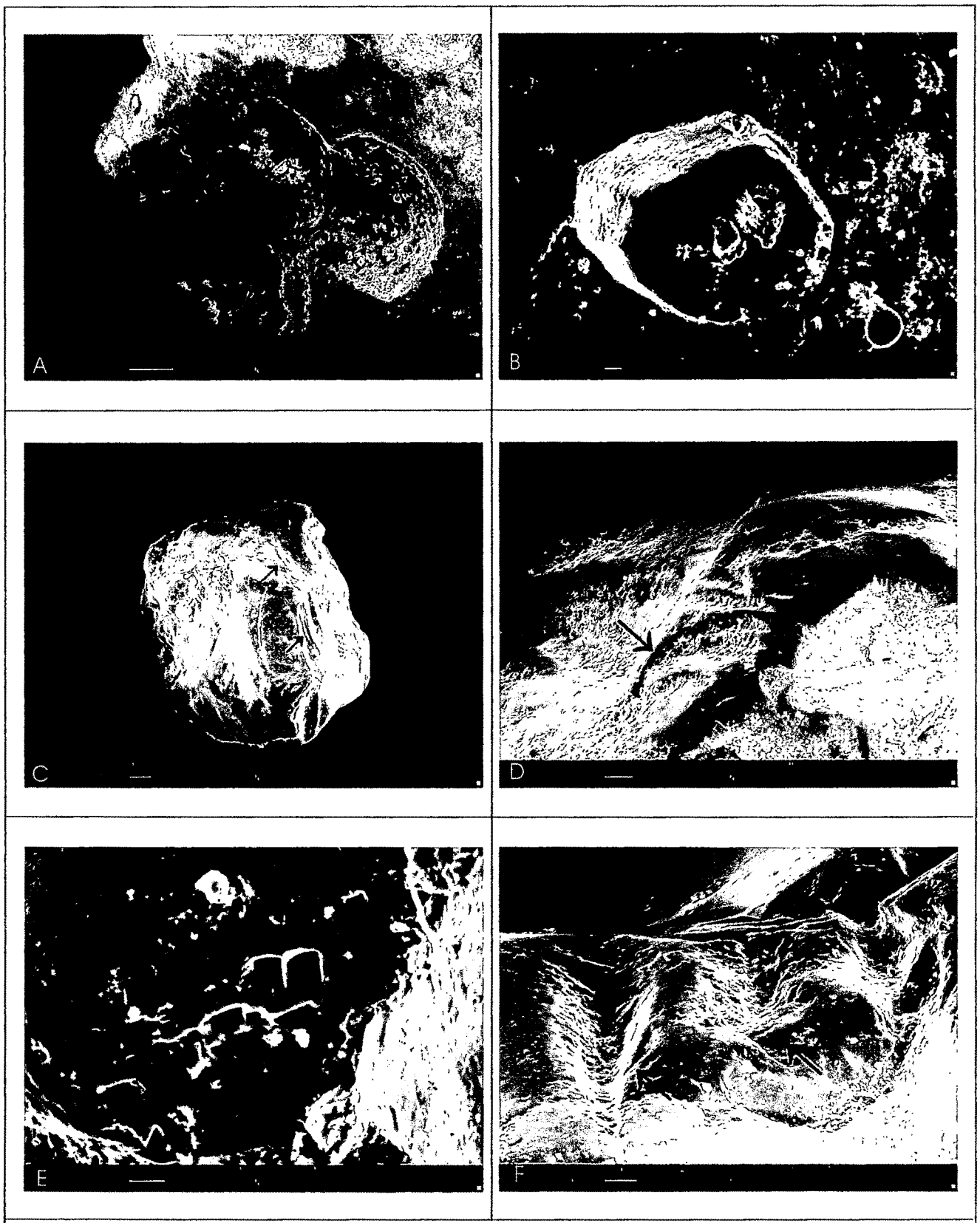

Fig. 6.21 - SEM Photomicrographs Showing The Surface Features Of Quartz Grains (Location - Mindhola River Sections) [A,B - Impact Features, C - Straight and Curved Steps, D - Conchoidal Fractures, E - Mechanically Formed "V"s, and F - Scratches and Grooves on the Surfaces of the Grains].

Sample No.	Surface Textures																		
	1	2	3	4	5	6	7	8	9	10	11	12	13	14	15	16	17	18	19
KmB1C	X	X	X	X	X	X	X	X	X		X	X		X	X	X			
KmB1F	X	X	X	X	X	X	X	X	X	X		X	X	X	X	X		X	X
KmB2A	X	X	X	X	X	X	X	X	X	X				X	X	X	X		X
KmB4D	X	X	X	X		X	X	X	X				X		X				
MB3A	X	X	X	X		X	X	X	X				X		X				
MB6C	X	X	X	X	X	X	X	X	X	X		X		X		X		X	X
MB5J	X	X	X	X	X	X	X	X	X			X		X	X	X			X
MB3F	X	X	X	X	X	X	X	X		X		X		X		X			X
MB4C	X	X	X	X	X	X	X	X		X				X		X		X	X
MB5E	X	X	X	X	X	X	X		X		X	X		X		X		X	X
MB7J	X	X	X	X	X	X	X	X	X	X		X		X		X		X	X
TB3A	X	X	X	X	X		X		X	X		X		X	X			X	X
TB3a	X	X		X		X	X	X	X			X		X	X		X	X	X
TB4E	X	X	X	X	X	X	X	X	X	X		X		X	X	X	X	X	X
TB2B	X	X	X	X	X	X	X	X	X	X		X		X		X		X	X
TB3B	X	X	X	X	X	X	X			X	X	X		X	X	X			
TB6C	X	X	X	X	X	X	X	X	X	X		X		X		X		X	X
TB5E	X	X	X	X	X	X	X	X		X		X		X	X			X	X
TB1B	X	X	X	X	X	X	X	X	X			X			X			X	
TB3e	X	X	X	X	X		X	X	X	X	X	X		X	X	X		X	X
																		(X – Present)	

Table 6.4 – Table Showing The Various Surface Textures Exhibited By The Quartz Grains.
{where, 1-Sub-Angularity, 2-Medium Relief, 3-Irregular Pits, 4-Conchoidal Fractures, 5-Straight Steps, 6-Arcuate Steps, 7-Straight Scratches, 8-Arcuate Scratches, 9-Mechanical V's, 10-Angular Outlines, 11-Rounded Outlines, 12-Friction Features (Impact Pit), 13-Polishing, 14-Breakage Blocks, 15-Coalescing Impact Pits, 16-Non-Coalescing Impact Pits, 17-Meandering Ridges, 18-Oriented Fractures, 19-Cleavage Planes.}

The features, which are commonly observed include, conchoidal fractures, coalescing irregular impact pits, straight and arcuate steps, straight and curved scratches, mechanically formed V's, friction features, breakage blocks and cleavage planes.

6.4 TRACE ELEMENT STUDIES

Trace elements are represented in both marine as well as fresh water environments, however their proportions vary and some of the associated trace elements are characteristically different in marine and the corresponding fresh water fractions (Keith & Degens, 1959). In the present study, trace element analysis has been opted for the Quaternary sediments to

acquire their relative concentrations, which in turn reflects the probable nature of the environments of their depositing medium.

In order to accomplish the above studies, sediment samples representing the different lithological units of a complete composite section have been analyzed using Atomic Absorption Spectrophotometer (GBC 906AA) and Shimadzu UV – 160A Spectrophotometer adopting the standard methods of Jefferey (1975) and Haas et al., (1984).

The results obtained from this analysis have been summarized in table 6.5, whereas figure 6.22 exhibits the vertical variation in the concentration of trace elements.

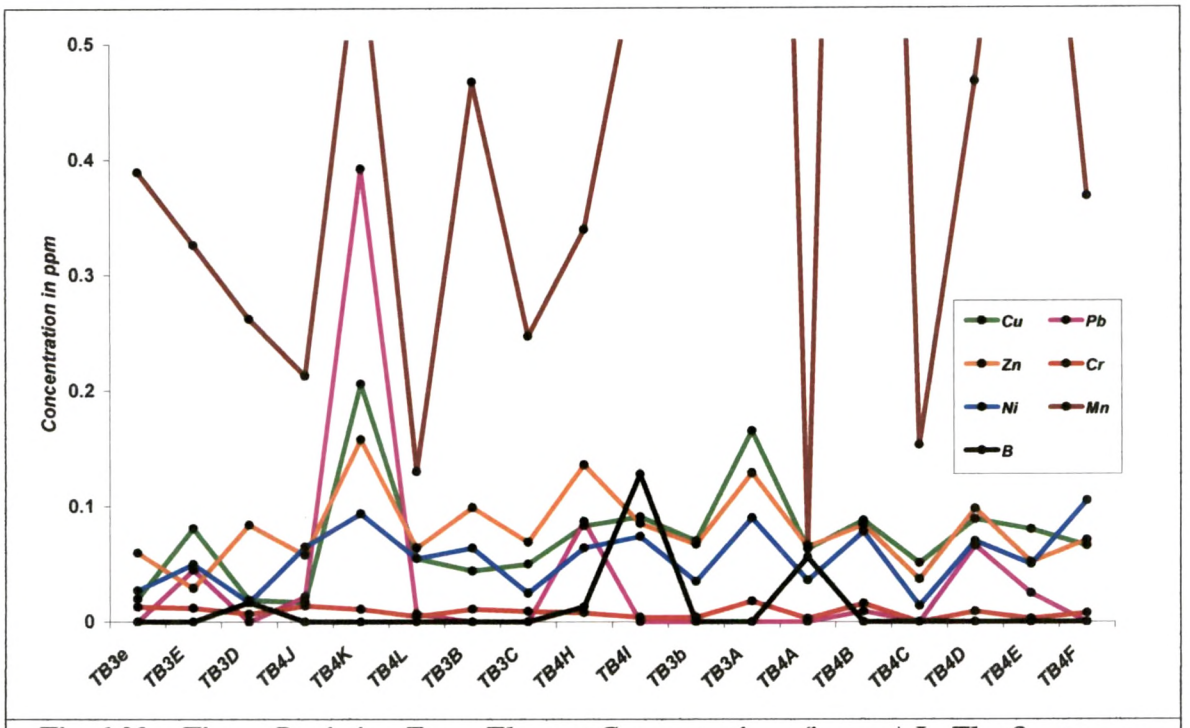

Fig. 6.22 – Figure Depicting Trace Element Concentrations (in ppm) In The Quaternary Sediments Belonging To Tapi River (Location: Puna And Dhatwa).

The results have shown that the concentration of Fe is comparatively higher as compared to other elements such as Copper (Cu), Lead (Pb), Zinc (Zn), Chromium (Cr), Nickel (Ni) and Manganese (Mn). However, Boron (B) is found to be practically absent in all the samples.

Sample	Trace Elements							
	Cu	Pb	Zn	Fe	Cr	Ni	Mn	B
TB3e	0.02	ND	0.06	9.035	0.013	0.027	0.389	ND
TB3E	0.081	0.045	0.029	12.734	0.012	0.05	0.326	ND
TB3D	0.019	ND	0.084	10.168	0.007	0.017	0.262	0.017
TB4J	0.017	0.022	0.058	14.542	0.014	0.065	0.213	ND
TB4K	0.206	0.392	0.158	21.27	0.011	0.094	0.596	ND
TB4L	0.055	0.007	0.064	9.146	0.005	0.055	0.13	ND
TB3B	0.044	ND	0.099	7.93	0.011	0.064	0.467	ND
TB3C	0.05	ND	0.069	11.354	0.009	0.025	0.247	ND
TB4H	0.083	0.087	0.136	18.642	0.008	0.064	0.339	0.013
TB4I	0.091	ND	0.085	10.356	0.004	0.074	0.585	0.128
TB3b	0.07	ND	0.067	3.696	0.004	0.035	0.65	ND
TB3A	0.165	ND	0.129	17.388	0.018	0.09	1.937	ND
TB4A	0.063	ND	0.065	11.756	0.003	0.036	0.066	0.056
TB4B	0.088	0.009	0.084	3.59	0.016	0.078	1.718	ND
TB4C	0.051	ND	0.037	11.252	ND	0.014	0.153	ND
TB4D	0.089	0.066	0.098	8.513	0.009	0.07	0.467	ND
TB4E	0.08	0.025	0.052	8.78	0.003	0.05	0.848	ND
TB4F	0.066	ND	0.071	13.416	0.008	0.105	0.368	ND

(Concentration in ppm)

Table 6.5 Trace Element Concentrations In The Quaternary Sediments Of The Study Area.

6.5 PALAEONTOLOGICAL STUDIES

In order to substantiate the results obtained from the various laboratory studies, an attempt has been made in the present work to bring about the detail information on the palaeontological aspects of the terrestrial Quaternary sediments of the study area. The critical observations made on the lithological successions have strongly indicated the absence of appreciable mega-fossil remains baring traces of broken shell fragments scattered within the sand and silt units at certain locations. Since these shells are highly disarticulated, broken and devoid of any significant morphological characters, they seem to have been transported and in no case represent their in-situ nature. Traces of microforms perhaps belonging to Ostracodes and Foraminifera (?) have been recoded under the microscope (Fig. 6.23). However, these shells are broken, highly worn out, devoid of any identifiable morphological characters and points to their transported and reworked nature, which makes it difficult for precise identification and to consider for overall interpretations.

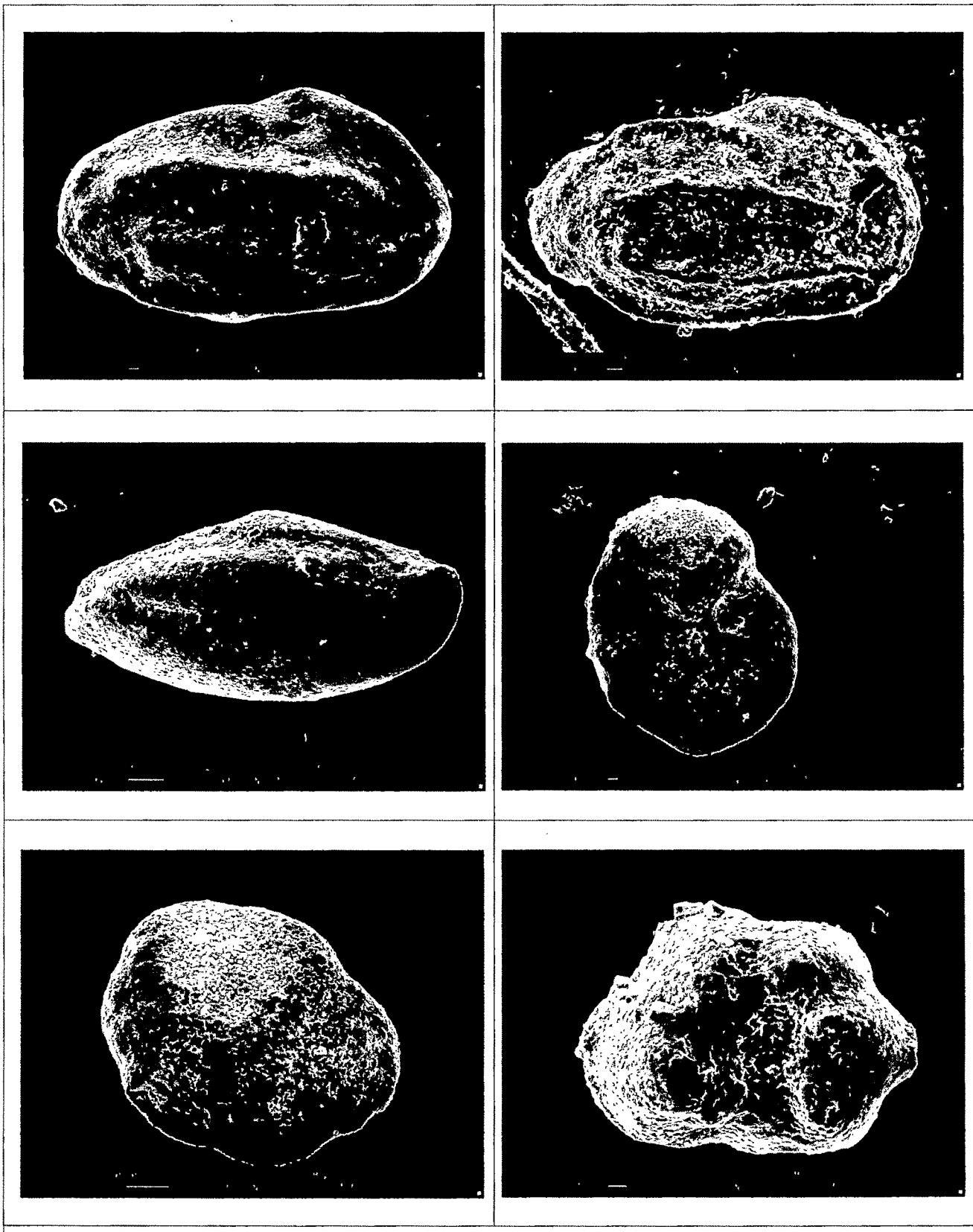

Fig. 6.23 - SEM Photomicrographs Showing The Microforms Recorded In The Quaternary Sediments Of Study Area.